ChemPubSoc Europe

DOI: 10.1002/chem.201405408

CHEMISTRY A European Journal Full Paper

Asymmetric Catalysis | *Hot Paper*

Enhancing Effects of Salt Formation on Catalytic Activity and Enantioselectivity for Asymmetric Hydrogenation of Isoquinolinium Salts by Dinuclear Halide-Bridged Iridium Complexes Bearing Chiral Diphosphine Ligands

Yusuke Kita, Kenta Yamaji, Kosuke Higashida, Kandula Sathaiah, Atuhiro Iimuro, and Kazushi Mashima*[a]

Abstract: Asymmetric hydrogenation of 1- and 3-substituted and 1,3-disubstituted isoquinolinium chlorides using triply halide-bridged dinuclear iridium complexes [{Ir(H)(diphosphine)}$_2$(μ-Cl)$_3$]Cl has been achieved by the strategy of HCl salt formation of isoquinolines to afford the corresponding chiral 1,2,3,4-tetrahydroisoquinolines (THIQs) in high yields and with excellent enantioselectivities after simple basic work-up. The effects of salt formation have been investigated by time-course experiments, which revealed that the generation of isoquinolinium chlorides clearly prevented formation of the catalytically inactive dinuclear trihydride complex, which was readily generated in the catalytic reduction of salt-free isoquinoline substrates. Based on mechanistic investigations, including by ^{1}H and ^{31}P{^{1}H} NMR studies and the isolation and characterization of several intermediates, the function of the chloride anion of the isoquinolinium chlorides has been elucidated, allowing us to propose a new outer-sphere mechanism involving coordination of the chloride anion of the substrates to an iridium dihydride species along with a hydrogen bond between the chloride ligand and the N-H proton of the substrate salt.

Introduction

Asymmetric hydrogenation of unsaturated organic compounds has been established as one of the most efficient synthetic methods for obtaining chiral substrates.[1] Among various unsaturated substrates, the asymmetric hydrogenation of heteroarenes, particularly N-heteroarenes such as pyridines, quinolines, isoquinolines, quinoxalines, pyrroles, and indoles, has attracted recent interest since this provides a straightforward route to a wide range of enantiomerically pure saturated N-heterocycles, which are abundant motifs in many biologically active compounds.[2] Since the pioneering work by Murata, who reported the asymmetric hydrogenation of 2-methylquinoxaline using an Rh/(*S*,*S*)-DIOP catalyst system,[3] development of this attractive reaction paradigm has been limited owing to the high stability of N-heteroarenes and the strong coordination ability of both N-heteroarenes and their hydrogenated N-heterocycles to the catalytically active metal center. Iridium complexes have typically been employed as effective catalysts for the asymmetric hydrogenation of N-heteroaromatics, although chiral ruthenium,[4] rhodium,[5] and palladium[6] complexes have also been shown to be effective. Concerning the iridium catalyst system, novel and efficient strategies have been developed through chemically activating catalysts as well as substrates for the successful asymmetric hydrogenation of N-heteroaromatics.[7] Most research approaches have been directed towards activating the catalysts.[8–10] The most common protocol is to add iodine or a halide-containing species such as 1-bromo-3-chloro-5,5-dimethylhydantoin to the catalyst precursors to oxidize Ir^{I} precursors to catalytically active Ir^{III} species.[11] The second approach is the addition of secondary amines that are converted to amido ligands that bind at the catalytically active iridium species through an outer-sphere mechanism.[12] On the other hand, activation of substrates has recently been targeted. Pre-activation of substrates by adding Brønsted acids such as HCl and trifluoroacetic acid (Scheme 1 a)[9d,13,14] and protecting agents such as benzyl halides and chloroformates to N-heteroaromatics (Scheme 1 b)[15] produces the corresponding salts, the aromaticity and coordination ability of which are thereby modified. Recently, we demonstrated that HX salts of quinolines, isoquinolines, and pyridines represented pre-activated substrates suitable for asymmetric hydrogenation, showing enhanced reactivity and/or enantioselectivity when using halide-bridged dinuclear iridium complex [{Ir(H)(diphosphine)}$_2$(μ-Cl)$_3$]Cl (**1**; Scheme 2) bearing chiral diphosphine ligands.[13] In this context, we directed our efforts towards delineating a mechanism to rationalize the enhanced catalytic activity and enantioselectivity in the asymmetric hydrogenation of N-het-

[a] *Dr. Y. Kita, K. Yamaji, K. Higashida, Dr. K. Sathaiah, A. Iimuro, Prof. Dr. K. Mashima*
Department of Chemistry, Graduate School of Engineering Science
Osaka University, CREST
Toyonaka, Osaka 560-8531 (Japan)
E-mail: mashima@chem.es.osaka-u.ac.jp

Supporting information for this article is available on the WWW under http://dx.doi.org/10.1002/chem.201405408.

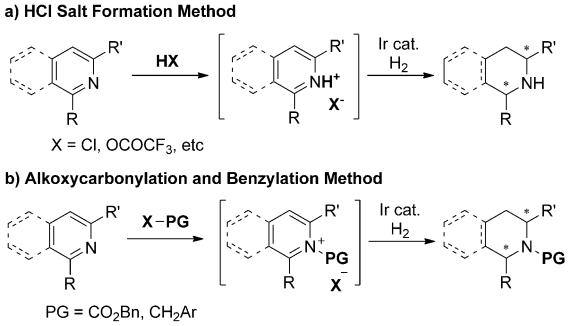

Scheme 1. Asymmetric hydrogenation of N-heteroaromatics through substrate activation by (a) the HX salt formation method and (b) the alkoxycarbonylation and benzylation method.

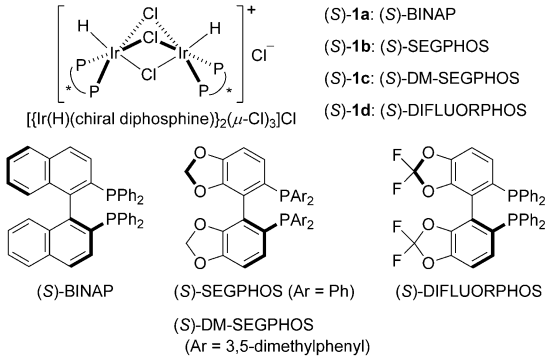

Scheme 2. Chiral dinuclear iridium complexes.

eroaromatics. For the present work, we selected isoquinolines as model substrates, which show clear effects of salt formation when catalyst **1** is used for asymmetric hydrogenation. Specifically, hydrogenation of 3-substituted isoquinolinium salts provides easier access to chiral 3-substituted 1,2,3,4-tetrahydroisoquinolines (THIQs) compared with other asymmetric hydrogenations of salt-free substrates[15c] as well as traditional synthetic methods,[16] and allows easy work-up by simple treatment with base to remove HX, as described in our previous report (Scheme 3).[13b] Moreover, isoquinolines have been regarded as some of the most challenging substrates for asymmetric hydrogenation.[15,17] Herein, we report full details of asymmetric

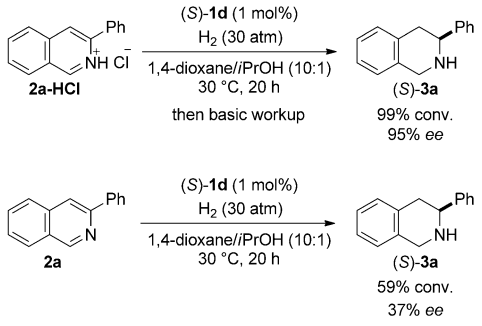

Scheme 3. Comparison of asymmetric hydrogenations of isoquinolinium salts and isoquinoline catalyzed by a dinuclear iridium complex.[13b]

hydrogenations of isoquinolinium salts, including a screening of counter anions of the salt substrates, the wider substrate scope, and mechanistic studies, in order to better understand the significant effects of the use of salt substrates.

Results and Discussion

Anion effects on asymmetric hydrogenation of isoquinolinium salts by a chloride-bridged dinuclear iridium catalyst (*S*)-1 a

With the aim of elucidating anion effects on the asymmetric hydrogenation of isoquinolinium salts, we first studied the reactions of various 3-phenylisoquinolinium salts (**2 a-HX**) catalyzed by a triply-chloride-bridged dinuclear iridium complex (*S*)-**1 a**. The reaction conditions were 30 atm H_2; 1,4-dioxane/isopropyl alcohol (10:1); 20 h; 30 °C, and the results are summarized in Table 1. We first examined the effects of chloride, bromide, and iodide anions using the same chloride catalyst

Table 1. Screening of counter anions in the asymmetric hydrogenation of **2 a-HX**.[a]

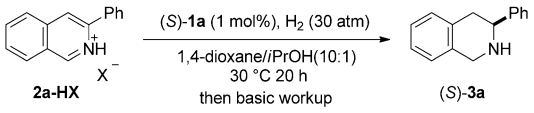

Entry	X	Conv.[b] (%)	*ee*[c] (%)
1	Cl	>99	85
2	Br	38	52
3	I	65	38
4	OTf	66	68
5	$OCOCF_3$	>99	73
6	OTs	98	84
7	NO_3	>99	84

[a] Reaction conditions: A mixture of 3-phenylisoquinolinium salt (0.24 mmol), (*S*)-**1 a** (2.4 μmol), and 1,4-dioxane/*i*PrOH (10:1, 3 mL), under H_2 (30 atm), was heated at 30 °C for 20 h. [b] Determined by ^{1}H NMR analysis. [c] Determined by HPLC analysis.

(*S*)-**1 a**, since we previously observed that the three bridging chloride ligands of (*S*)-**1 a** remained intact and did not undergo halide-exchange with HBr and HI or with bromide and iodide salt substrates.[13a] Asymmetric hydrogenation of **2 a-HCl** followed by basic work-up afforded the corresponding product (*S*)-**3 a** with >99% conversion and 85% *ee* (entry 1), whereas asymmetric hydrogenations of **2 a-HBr** and **2 a-HI** resulted in lower conversions and rather low enantioselectivities (entries 2 and 3). The triflic acid (TfOH) salt of 3-phenylisoquinoline (**2 a-HOTf**) was hydrogenated with moderate conversion and 68% *ee* (entry 4), and the trifluoroacetic acid (TFA) salt was fully hydrogenated to give the product with 73% *ee* (entry 5). Notably, the tosylate (**2 a-HOTs**) and nitrate (**2 a-HNO_3**) were suitable substrates to produce (*S*)-**3 a** with high enantioselectivity (84% *ee*) (entries 6 and 7), almost matching that with **2 a-HCl**. Thus, enantioselectivity was affected by the counter anion of the isoquinolinium salts, and we selected the HCl salt as the best in

terms of its high conversion and enantioselectivity as well as its ease of handling and simple product recovery by basic work-up.

Substrate scope for asymmetric hydrogenation of isoquinolinium chlorides

We checked the generality of the salt formation strategy in asymmetric hydrogenations of 3-substituted and 1-substituted isoquinolinium chlorides using iridium complex (*S*)-**1 d** bearing (*S*)-DIFLUORPHOS as a catalyst in a solvent of 1,4-dioxane/isopropyl alcohol (10:1).[13b] We have previously reported the scope of the asymmetric hydrogenation of 3-substituted isoquinolinium chlorides, as outlined in Equation (1).[13b] 3-Aryl-substituted substrates were hydrogenated with high enantioselectivity regardless of the electronic effect of substituents on the phenyl group. In the case of sterically congested substrates, moderate enantioselectivity was observed. In addition, isoquinolinium chlorides bearing benzyl and cyclohexyl groups were also good substrates for the asymmetric hydrogenation.

We found that 1-aryl isoquinolinium chlorides could be hydrogenated under relatively harsh conditions (80 °C) to afford the desired products with excellent enantiomeric excesses, some of which have been reported previously (Table 2). 1-Aryl-substituted substrates were efficiently hydrogenated regardless of the electronic effect of the substituents on the phenyl group (entries 2–6). On the other hand, steric effects of *ortho* substituents affected the reaction rate. 2-Chlorophenylisoquinolinium chloride required 28 h to reach 94% conversion (entry 7). The high functional group tolerance of the process was demonstrated by the successful use of an isoquinoline bearing a bromo substituent (entry 8). Moreover, hydrogenations of 1-alkyl isoquinolinium salts proceeded efficiently (entries 9–11), although a benzyl-substituted substrate **2 p-HCl** required a change of catalyst to one bearing (*S*)-DM-SEGPHOS (entry 9).

We then turned our attention to asymmetric hydrogenation of 1,3-disubstituted isoquinolinium chlorides to produce two stereogenic centers at the 1,3-positions, as this would represent an advantageous feature of our asymmetric hydrogenation protocol for heteroaromatics.[11f,18] Table 3 shows the results of hydrogenations of several 1,3-disubstituted isoquinolinium salts under the optimized conditions. The asymmetric hydrogenation of 1,3-diphenyl substrate **4 a-HCl** has been reported previously, yielding only one isomer of THIQ (1*S*,3*S*)-**5 a** in 93% conversion with 98% *ee* with complete *syn*-selectivity (entry 1). The ^{1}H NMR spectrum of (1*S*,3*S*)-**5 a** showed signals due to a single diastereomer, and the absolute configuration of this product was determined by X-ray crystallographic analysis of its 4-bromobenzoyl derivative. 1,3-Diaryl-, 1-aryl-3-alkyl-, and 1-alkyl-3-aryl-substituted isoquinolinium chlorides proved to be good substrates for the present catalytic system (entries 2–6). Lower conversion was observed for **4 d-HCl**, presumably due to weak basicity of the sp^2-nitrogen owing to the presence of two electron-withdrawing groups, resulting in easy dissociation of HCl from its isoquinolinium salt. Enantioselectivity was only slightly affected by the electronic nature and position of the substituents on the aromatic substrates. Substituents at the 6- and 7-positions had no effect on the reactivity or enantioselectivity (entries 7–10). In all reactions, no peaks due to a minor isomer could be detected in the ^{1}H NMR spectra of the products, suggesting high diastereoselectivity (*syn*-selectivity based on (1*S*,3*S*)-**5 a**).

Other disubstitution patterns were also amenable to this catalytic reaction. The reaction of 3,4-diphenylisoquinolinium chloride **6-HCl** gave the corresponding hydrogenated product with 43% *ee*, and only the *syn* isomer was obtained [Eq. (2)]. 1,4-Diphenylisoquinolinium chloride **8-HCl** was hydrogenated to afford a 4:1 mixture of *syn* and *anti* isomers with high enantioselectivities [Eq. (3)]. Stereochemistries observed in the asymmetric hydrogenation of **6-HCl** and **8-HCl** were rationalized by assuming a tautomerization between an imine form

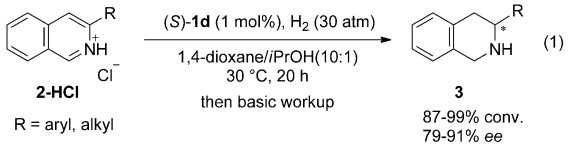

Table 2. Asymmetric hydrogenation of 1-substituted isoquinolinium salts.[a]

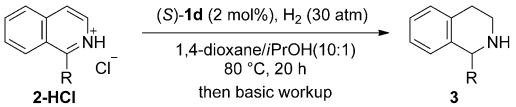

Entry	R		Conv.[b] (%)	*ee*[c] (%)	
1	phenyl	**3 h**	99	96 (*S*)	Ref. [13b]
2	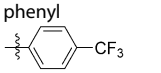	**3 i**	99	98 (+)	Ref. [13b]
3	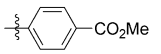	**3 j**	98[d]	97 (+)	this work
4	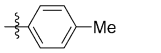	**3 k**	98[d]	97 (+)	this work
5	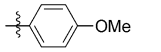	**3 l**	99	99 (*S*)	Ref. [13b]
6	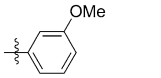	**3 m**	98[d]	96 (−)	this work
7[e]	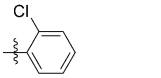	**3 n**	94[d]	96 (*R*)	this work
8	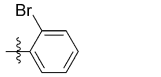	**3 o**	75	96 (*R*)	Ref. [13b]
9[f]		**3 p**	63	85 (*S*)	Ref. [13b]
10	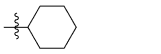	**3 q**	99	79 (−)	Ref. [13b]
11		**3 r**	98	91 (*S*)	Ref. [13b]

[a] Reaction conditions: A mixture of isoquinolinium salt (0.24 mmol), (*S*)-**1 d** (4.8 μmol), and 1,4-dioxane/*i*PrOH (10:1, 3 mL), under H_2 (30 atm), was heated at 80 °C for 20 h. [b] Determined by ^{1}H NMR analysis. [c] Determined by HPLC analysis. [d] Isolated yield. [e] Run for 28 h. [f] 4.8 μmol of [{Ir(H)[(*S*)-DM-segphos]}$_2$(μ-Cl)$_3$]Cl [(*S*)-**1 c**] was used as catalyst.

Table 3. Asymmetric hydrogenation of 1,3-disubstituted isoquinolinium salts.[a]

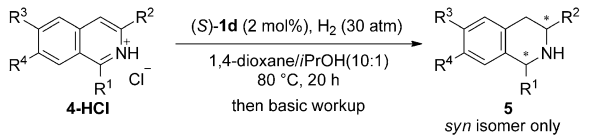

Entry	R^1	R^2	R^3	R^4		Yield[b] (%)	*ee*[c] (%)
1[d]	phenyl	phenyl	H	H	**5a**	93	98 (*S*, *S*)
2	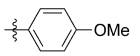	phenyl	H	H	**5b**	91	96 (+)
3	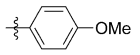	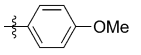	H	H	**5c**	93	98 (−)
4[e]	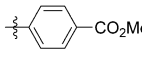	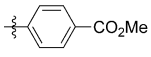	H	H	**5d**	56	91 (+)
5		phenyl	H	H	**5e**	87	97 (−)
6	phenyl	*n*-hexyl	H	H	**5f**	80	98 (−)
7	phenyl	phenyl	H	F	**5g**	89	94 (+)
8	phenyl	phenyl	H	OMe	**5h**	88	92 (−)
9	phenyl	phenyl	F	H	**5i**	89	94 (+)
10	phenyl	phenyl	CH_3	H	**5j**	87	97 (+)

[a] Reaction conditions: A mixture of isoquinolinium salt (0.24 mmol), (*S*)-**1d** (4.8 μmol), and 1,4-dioxane/*i*PrOH (10:1, 3 mL), under H_2 (30 atm), was heated at 80 °C for 20 h. [b] Isolated yield. [c] Determined by HPLC analysis. [d] Ref. [13b]. [e] Catalyst loading was 5 mol% and run at 120 °C.

and an enamine form of the dihydroisoquinolinium salt, a half-reduced intermediate compound, which would be consistent with our previous deuterium-labeling experiments.[13b] As shown in Scheme 4 for 3,4-disubstituted isoquinoline, rapid tautomerization provided equimolar amounts of enantiomers of the imines, subsequent hydrogenation of which proceeded against the substituent at the C4 position to selectively form the *syn* isomer. On the other hand, as shown in Scheme 5, the reduction of the 1,4-disubstituted isoquinolinium salt **8-HCl** initially induced chirality at the C1 position with high enantioselectivity, as described in our previous report.[13b] Subsequent tautomerization provided a mixture of *syn* and *anti* isomers of

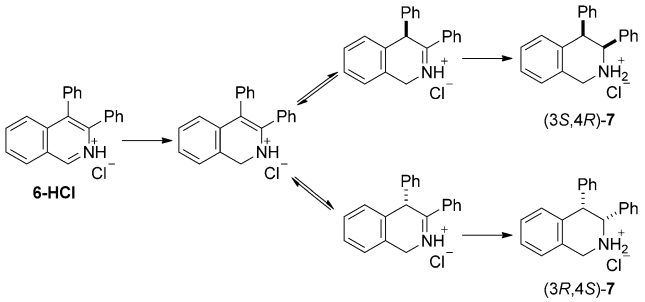

Scheme 4. Reaction pathways in asymmetric hydrogenation of **6-HCl**.

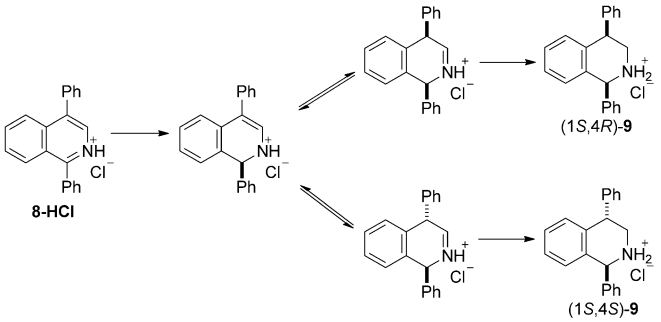

Scheme 5. Reaction pathways in asymmetric hydrogenation of **8-HCl**.

the imine, and the second reduction determined the ratio of the *syn* and *anti* isomers of the 1,2,3,4-tetrahydroisoquinolinium salts. In the second reduction, the difference between the two transition states was considered to be small, resulting in low diastereoselectivity.

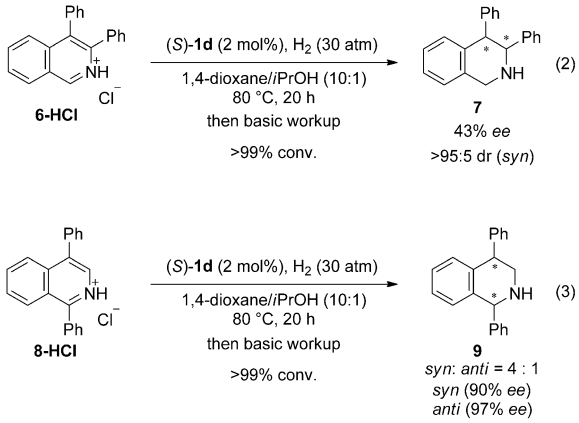

Time-course study on asymmetric hydrogenation of isoquinoline 2a and isoquinolinium chloride 2a-HCl

In order to reveal the effects of salt formation on the asymmetric hydrogenation of isoquinolines catalyzed by iridium dinuclear complexes, we performed time-course studies on such reactions of **2a** and **2a-HCl** under the optimized conditions. Plots of the yield of **3a** against time showed that the reaction of **2a-HCl** proceeded steadily, reaching a yield of 99% after 20 h, whereas the reaction of **2a** was rather slow (Figure 1a). This difference could be attributed to whether or not the hy-

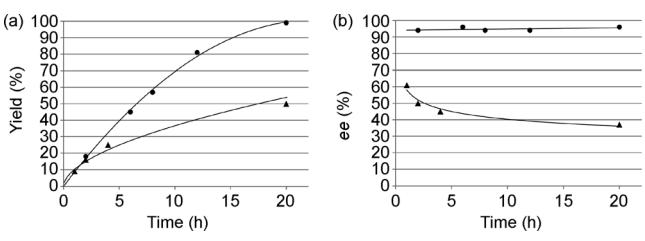

Figure 1. Time courses of yield (a) and enantiomeric excess (b) of **3a** in asymmetric hydrogenations of **2a** (triangles) and **2a-HCl** (circles) catalyzed by (*S*)-**1d**.

drogenated product could coordinate to the iridium center. It is noteworthy that the enantiomeric excess of **3a** after basic work-up remained unaltered during the course of the reaction of **2a-HCl**, whereas it decreased during the course of the reaction of **2a** (Figure 1b). This decrease in *ee* during the reaction of **2a** can be rationalized in terms of a change in the active species induced by the hydrogenated product. However, such negative effects of amine formation are as yet unclear, although we previously reported that the hydrogenated products from 2-substituted quinoxalines afforded the corresponding amide-hydride species, which served as catalysts in an outer-sphere mechanism.[12] These experiments clearly showed that salt formation inhibited the negative effects of the product amines on both reactivity and enantioselectivity.

Synthesis and reactions of anionic mononuclear iridium complexes

The time-course experiments suggested that the activity and enantioselectivity of the iridium catalyst were highly dependent on whether or not the product could coordinate to the metal center. We thus conducted control experiments to elucidate any interaction of (*S*)-**1a** with 3-phenylisoquinoline (**2a**) and its hydrogenated product (*S*)-**3a** together with their HCl salts. As outlined in Scheme 6, since these mixtures were in equilibrium and no adducts could be isolated, we used 10 equivalents of each substrate in order to shift the equilibrium to the adducts as much as possible. When (*S*)-**1a** and 10 equivalents of **2a** were dissolved in CD_2Cl_2 at room temperature, we observed a new hydride peak centered at $\delta = -18.3$ ppm (br s) in the ^{1}H NMR spectrum and two signals at $\delta = 2.8$ (br) and -5.3 ppm (br) in the $^{31}P\{^1H\}$ NMR spectrum. This suggested that an isoquinoline-coordinated complex (*S*)-**10** was generated, based on comparison with signals observed for the 2-phenylquinoxaline-coordinated iridium complex (*S*)-**15** [major: $\delta_H = -18.2$ ppm (dd, $J_{H\text{-}P} = 12.3$, 17.2 Hz); $\delta_P = -5.9$ (d, $J_{P\text{-}P} = 19.4$ Hz) and -12.9 ppm (d, $J_{P\text{-}P} = 19.4$ Hz); minor: $\delta_H = -19.3$ ppm (dd, $J_{H\text{-}P} = 14.2$, 21.7 Hz); $\delta_P = 2.2$ (d, $J_{P\text{-}P} = 19.4$ Hz) and -4.3 ppm (d, $J_{P\text{-}P} = 19.4$ Hz)].[12] Similarly, (*S*)-3-phenyl-1,2,3,4-tetrahydroisoquinoline [(*S*)-**3a**] (95% *ee*) was found to coordinate to the iridium center in CD_2Cl_2 to form complex (*S*)-**11**, which was spectroscopically characterized. The ^{1}H NMR spectrum featured a double doublet centered at $\delta = -19.5$ ppm ($J_{H\text{-}P} = 17.6$, 15.2 Hz) and the $^{31}P\{^1H\}$ NMR spectrum showed two doublets centered at $\delta = 3.2$ ($J_{P\text{-}P} = 19.4$ Hz) and -3.1 ppm ($J_{P\text{-}P} = 19.4$ Hz), these peaks being comparable to those found for the 4-methoxyaniline-coordinated iridium complex (*S*)-**16** [$\delta_H = -20.1$ ppm (dd, $J_{H\text{-}P} = 14.2$, 21.4 Hz); $\delta_P = 0.3$ (d, $J_{P\text{-}P} = 18.6$ Hz) and -5.6 ppm (d, $J_{P\text{-}P} = 18.6$ Hz)].[12] In sharp contrast to these neutral substrates, the reaction of (*S*)-**1a** and 10 equivalents of **2a-HCl** gave a facial mononuclear iridium trichloride-hydride complex (*S*)-**12**, which displayed a double doublet hydride signal centered at $\delta = -21.0$ ppm ($J_{H\text{-}P} = 19.9$, 14.9 Hz) and two doublets centered at $\delta = -0.36$ ($J_{P\text{-}P} = 18.3$ Hz) and -4.4 ppm ($J_{P\text{-}P} = 18.3$ Hz) in its $^{31}P\{^1H\}$ NMR spectrum. Notable inertness of the hydride species (*S*)-**12** toward **2a-HCl** was observed, as evidenced by the absence of

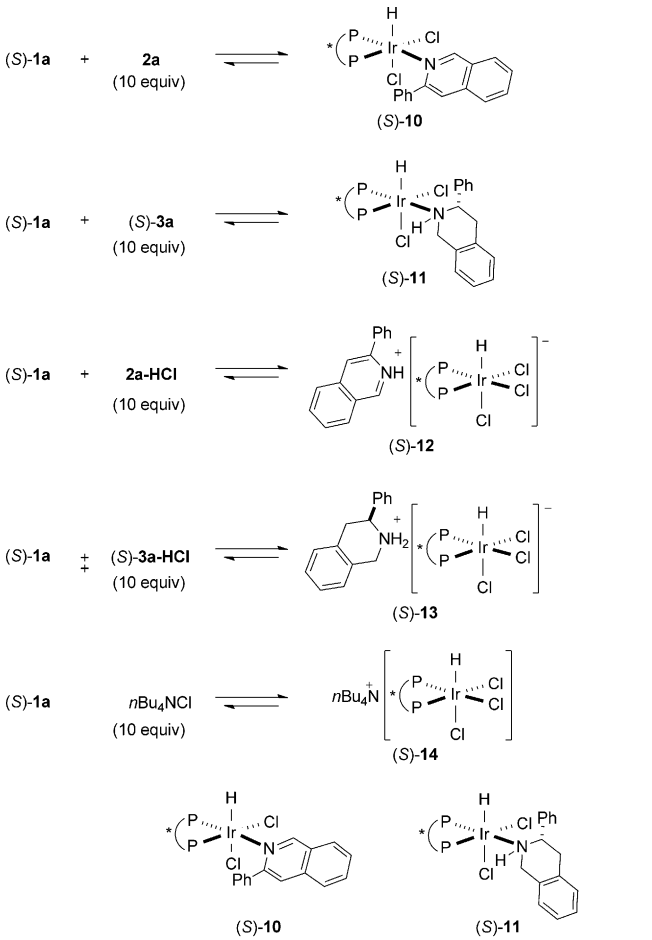

	(*S*)-**10**	(*S*)-**11**
^{1}H NMR (CD_2Cl_2, 400 MHz, 30 °C)	-18.3 (brs)	-19.5 (dd, $J_{H\text{-}P}$ = 17.6, 15.2 Hz)
$^{31}P\{^1H\}$ NMR (CD_2Cl_2, 161 MHz, 30 °C)	2.8 (br), -5.3 (br)	3.2 (d, $J_{P\text{-}P}$ = 19.4 Hz), -3.1 (d, $J_{P\text{-}P}$ = 19.4 Hz)

	(*S*)-**12**	(*S*)-**13**
^{1}H NMR (CD_2Cl_2, 400 MHz, 30 °C)	-21.0 (dd, $J_{H\text{-}P}$ = 19.9, 14.9 Hz)	-21.1 (t, $J_{H\text{-}P}$ = 18.2 Hz)
$^{31}P\{^1H\}$ NMR (CD_2Cl_2, 161 MHz, 30 °C)	-0.36 (d, $J_{P\text{-}P}$ = 18.3 Hz), -4.4 (d, $J_{P\text{-}P}$ = 18.3 Hz)	-0.19 (d, $J_{P\text{-}P}$ = 18.2 Hz), -4.6 (d, $J_{P\text{-}P}$ = 18.2 Hz)

(*S*)-**14**

^{1}H NMR (CD_2Cl_2, 400 MHz, 30 °C)	-20.6 (dd, $J_{H\text{-}P}$ = 19.1, 14.1 Hz)
$^{31}P\{^1H\}$ NMR (CD_2Cl_2, 161 MHz, 30 °C)	0.30 (d, $J_{P\text{-}P}$ = 17.7 Hz), -3.3 (d, $J_{P\text{-}P}$ = 17.7 Hz)

Scheme 6. Controlled reactions of (*S*)-**1a** with amines or ammonium salts.

peaks due to a hydrogenated product in the ^{1}H NMR spectrum. The ^{1}H NMR spectrum of a mixture of (*S*)-**1a** and 10 equivalents of **3a-HCl** in CD_2Cl_2 showed the same pattern as that of **12**. The chemical shifts and $J_{P\text{-}H}$ coupling constants of a hydride signal centered at $\delta = -21.1$ ppm (t, $J_{H\text{-}P} = 18.2$ Hz) and phosphorus signals centered at $\delta = -0.19$ (d, $J_{P\text{-}P} = 18.2$ Hz) and -4.6 ppm (d, $J_{P\text{-}P} = 18.2$ Hz) were in good accord with those of (*S*)-**12**, suggesting that an anionic iridium complex (*S*)-**13** similar to (*S*)-**12** except for the different cationic part was generated. The formation of anionic trichloro iridium complexes (*S*)-**12** and (*S*)-**13** was further supported by an experiment in which a mixture of 10 equivalents of tetrabutylammonium chloride and (*S*)-**1a** in CD_2Cl_2 afforded the corresponding anionic complex (*S*)-**14**, the ^{1}H NMR spectrum of which showed a hydride signal at $\delta = -20.6$ ppm (dd, $J_{H\text{-}P} = 19.1$, 14.1 Hz) and two phosphorus signals at $\delta = 0.30$ (d, $J_{P\text{-}P} = 17.7$ Hz) and -3.3 ppm (d, $J_{P\text{-}P} = 17.7$ Hz). In sharp contrast to nBu$_4$NCl, no new hydride peak appeared upon adding nBu$_4$NBF$_4$ or nBu$_4$NNO$_3$ to (*S*)-**1a** in CD_2Cl_2 (see the Supporting Information). As the anionic complexes **12**–**14** showed almost the same NMR spectral data, it was assumed that there was a hydrogen bond between N-H and a chloride ligand at the iridium center. Indeed, Esteruelas et al. reported that an anionic trichloro iridium complex **17** had a hydrogen bond between the chloride of the anionic iridium moiety and the hydrogen atom of the benzo[*h*]quinolinium cation,[19] and two hydrogen bonds between Et_2NH_2Cl and the chloride ligands of each ruthenium atom were reported to stabilize an anionic dinuclear triply-chloride-bridged ruthenium complex (*R*)-**18** bearing chelating diphosphine ligands (Figure 2).[20]

With the anionic iridium complexes (*S*)-**12** and (*S*)-**13** as well as neutral nitrogen-coordinated iridium complexes (*S*)-**10** and (*S*)-**11** in hand, solutions of these complexes in CD_2Cl_2 were exposed to molecular hydrogen (1 atm) for 18 h at room temperature and monitored by NMR spectroscopy. Monitoring the reaction of in situ generated complex (*S*)-**12** with H_2, (*S*)-**13** was observed along with the tetrahydroisoquinolinium salt after 1 week (Scheme 7). In contrast, exposure of (*S*)-**10** to hydrogen proceeded differently from that of (*S*)-**12**, affording the trihydride dinuclear complex (*S*)-**19**, which was reported to be catalytically inactive (Scheme 8).[12] Similar results were obtained for the reaction of the product-coordinated complex (*S*)-**11**. It should be emphasized that complex (*S*)-**13** did not react with H_2, whereas complex (*S*)-**11** reacted with H_2 to give the trihydride complex (*S*)-**19**. This clear reactivity difference between an anionic iridium complex and a neutral nitrogen-coordinated complex is consistent with the observed lower conversion (59%) of **2a** compared to that of its HCl salt (full conversion) under the catalytic conditions using (*S*)-**1a** (Scheme 1). Moreover, it was pointed out that the trihydride complex (*S*)-**19** reacted with the salt **2a-HCl** to regenerate a mixture of (*S*)-**1a** and (*S*)-**12** in 49% conversion (Scheme 9), whereas the reaction of (*S*)-**19** with **3a-HCl** did not regenerate a mixture of (*S*)-**1a** and (*S*)-**13**. Thus, before complete consumption of the HCl salt of 3-phenylisoquinoline **2a-HCl**, the deactivation process of the catalytic reaction could be suppressed by **2a-HCl** through its reactivation of the catalytically inactive trihydride complex (*S*)-**19**, if generated during the hydrogenation.

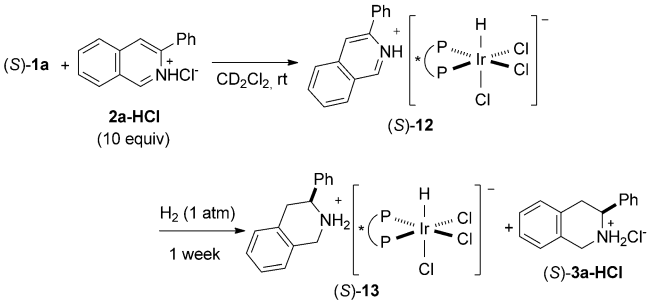

Scheme 7. Reaction of in situ generated (*S*)-**12** with H_2.

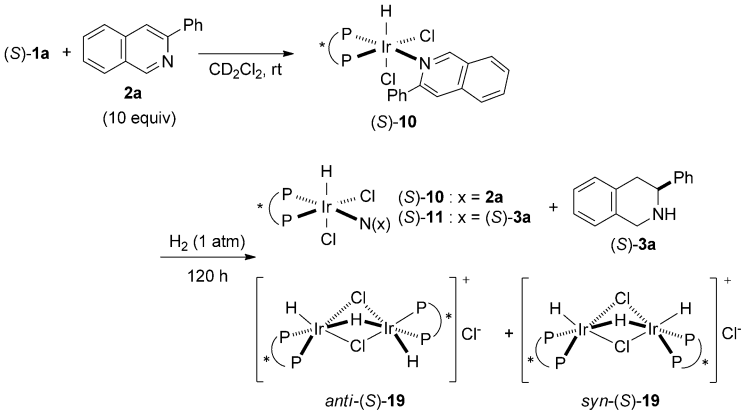

Scheme 8. Reaction of in situ generated (*S*)-**10** with H_2.

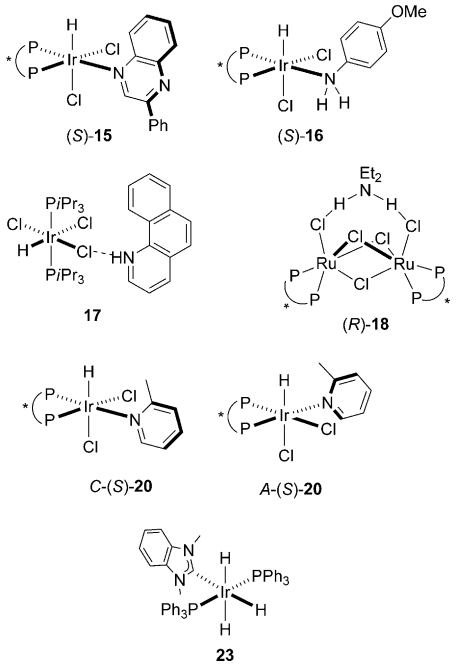

Figure 2.

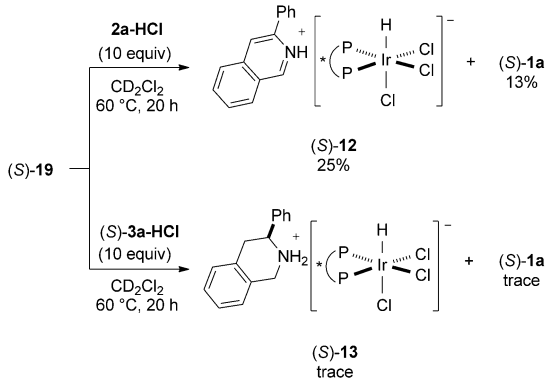

Scheme 9. Regeneration of (*S*)-**1 a** and the anionic complex from trihydride complex (*S*)-**19** by addition of isoquinolinium or ammonium salt.

Synthesis and reactivity of a dihydride iridium complex

We confirmed above that coordination of the chloride anion of isoquinolinium chloride formed an anionic iridium complex (*S*)-**12**, which could not hydrogenate **2 a-HCl** directly in the absence of H_2. Next, we conducted control experiments to identify any catalytically active species in the present asymmetric hydrogenation of isoquinolinium salts. We have previously proposed an iridium dihydride complex as a catalytically active complex for the asymmetric hydrogenation of quinoxalines.[12] Thus, we performed the controlled reaction of (*S*)-**1 a** with H_2 in the presence of α-picoline as a model donor ligand (Figure 3). When (*S*)-**1 a** and 10 equivalents of α-picoline were dissolved in CD_2Cl_2 at room temperature, we observed new hydride peaks centered at $\delta = -18.7$ (dd, $J_{H\text{-}P} = 17.1$, 13.0 Hz) and −19.9 ppm (dd, $J_{H\text{-}P} = 22.0$, 14.3 Hz) with relative intensities of 78:22 in the ^{1}H NMR spectrum. This suggested that two isomers of α-picoline-coordinated complexes (*S*)-**20** (Figure 2) were generated and assigned as *C*-(*S*)-**20**, (major) and *A*-(*S*)-**20**, (minor) based on the crystal structure of the previously reported complex (*S*)-**16**.[12] After 1 h under H_2 atmosphere, the signals due to (*S*)-**20** decreased, and new hydride peaks centered at $\delta = -9.40$ (ddd, $J_{H\text{-}H} = 3.5$ Hz, $J_{H\text{-}P} = 159.7$, 15.6 Hz) and −21.2 ppm (td, $J_{H\text{-}H} = 3.6$ Hz, $J_{H\text{-}P} = 15.0$ Hz) appeared. These could be assigned to the desired iridium dihydride complex (*S*)-**21** as a single stereoisomer. This may provide a rationale for the high enantioselectivity, even though the precursor dichlorides (*S*)-**20** consisted of two isomers. The aforementioned coupling constants suggested that one hydride ligand was oriented *trans* to one phosphine ligand and *cis* to the other, whereas the second hydride ligand was oriented *cis* to both phosphine ligands (Figure 2). Because (*S*)-**21** could not be isolated from the reaction mixture due to low conversion even after 25 h, we utilized a reported synthetic method for iridium dihydride complexes involving the reaction of an Ir^I complex with H_2 in the presence of donor ligands.[21] In fact, the reaction of in situ generated [IrCl((*S*)-binap)]$_2$ with H_2 (1 atm) in the presence of α-picoline in toluene at room temperature afforded the same iridium dihydride complex (*S*)-**21**, the hydride peaks of which were superimposed on those observed for the reaction of (*S*)-**1 a** with H_2 (Eq. (4)). In order to isolate crystals for a crystallographic study, we conducted a similar reaction of an Ir^I complex bearing SEGPHOS, [IrCl((*S*)-segphos)]$_2$, with *p*-methoxypyridine to afford a complex (*S*)-**22**, which was characterized by NMR spectroscopy [$\delta_H = -8.61$ (dd, $J_{P\text{-}H} = 18$, 160 Hz), −21.3 ppm (t, $J_{P\text{-}H} = 16$ Hz); $\delta_P = 8.13$, 0.30 ppm] and X-ray analysis. Figure 4 shows an ORTEP drawing of (*S*)-**22**, in which the iridium atom is seen to adopt an octahedral geometry. The overall structure of the dihydride based on NMR spectroscopy was clearly confirmed.

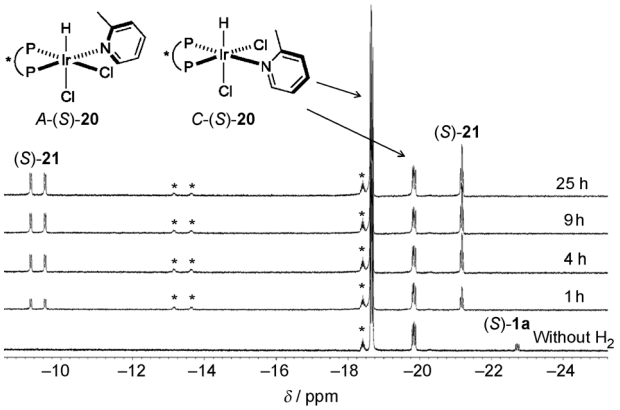

Figure 3. Time-dependent ^{1}H NMR spectra of hydride species in the reaction of (*S*)-**1 a** and α-picoline (10 equiv) under H_2 (1 atm) at room temperature. Asterisks indicate peaks due to an unidentified species.

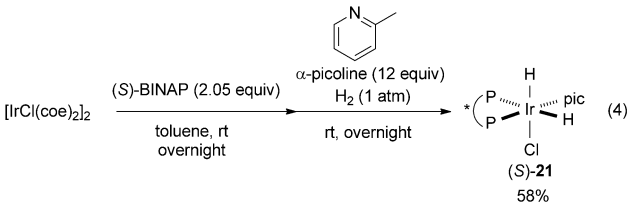

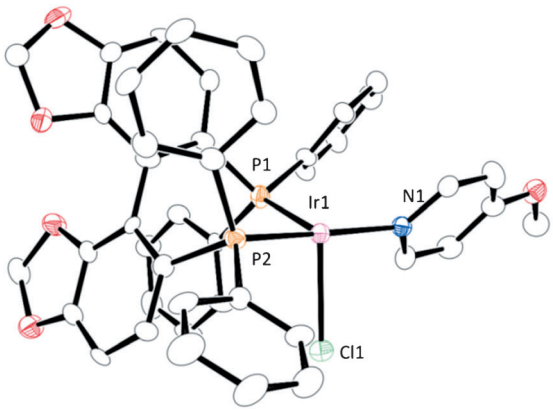

Figure 4. Crystal structure of (*S*)-**22** (hydrogen atoms omitted for clarity). Selected bond lengths [Å] and angles [°]: Ir1–P1 2.232(2), Ir1–P2 2.345(2), Ir1–Cl1 2.511(2), Ir1–N1 2.143(6); P1-Ir1-P2 93.48(8), P2-Ir1-N1 91.74(18), P2-Ir1-N1 173.82(19).

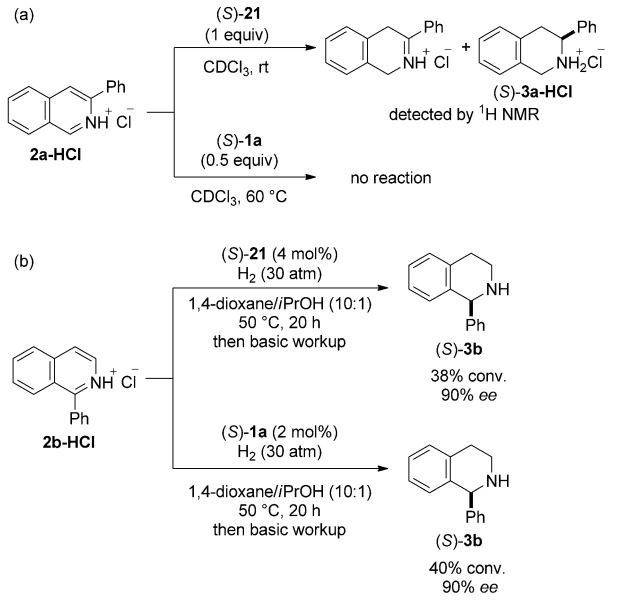

Scheme 10. Comparison of the efficacies of (*S*)-**21** and (*S*)-**1a** in (a) hydride attack on **2a-HCl** and (b) asymmetric hydrogenation of **2b-HCl**.

As shown in Scheme 10a, we compared the stoichiometric reactions with **2a-HCl** of the isolated dihydride complex (*S*)-**21** and the dinuclear iridium complex (*S*)-**1a** in the absence of H_2. Complex (*S*)-**21** showed high reactivity for the insertion of the isoquinolinium salt into the Ir–H bond to afford dihydro- and tetrahydroisoquinolinium salts, whereas (*S*)-**1a** showed no activity. Under milder conditions, these complexes were tested as catalysts for the asymmetric hydrogenation of **2b-HCl** under an H_2 pressure of 30 atm (Scheme 10b). The dihydride iridium complex (*S*)-**21** displayed almost the same activity and selectivity for the asymmetric hydrogenation of 1-substituted isoquinolinium salts as seen in the reaction using (*S*)-**1a**. This suggests that the dihydride complex could be involved in the catalytic cycle, although the isolated dihydride had picoline as a stabilizing ligand. Based on the observations that: (i) the chloride anion from substrates and products coordinated to the mononuclear iridium center to form mononuclear anionic complexes, (ii) the enantiomeric excess was sensitively affected by the counter anions of substrate salts, and (iii) another possible mononuclear trihydride iridium complex **23** (Figure 5), which was reported as an active species in the hydrogenation of quinolines,[22] was not observed in the reaction of (*S*)-**1a** with H_2, we conclude that the dihydride complex was probably coordinated by chloride to form a key intermediate for the hydrogenation of the isoquinolinium salts.

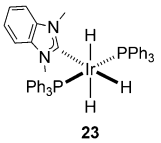

Figure 5. Trihydride iridium complex.[22]

Proposed mechanism for asymmetric hydrogenation of isoquinolinium salts

Scheme 11 shows the proposed catalytic cycle. The iridium dinuclear complex (*S*)-**1**, which is in equilibrium with the anionic iridium complex **A**, dissociates to allow coordination by the solvent.[12] The monohydride complex **B** is then formed, which can react with H_2 to form dihydride complex **C** with concomitant formation of HCl. Displacement of the solvent by the chloride could then occur to form the anionic dihydride complex **D**. Subsequent hydride attack on the isoquinolinium salt regenerates the monohydride complex **B** along with the dihydroisoquinoline, which is trapped with HCl to form the dihydroisoquinolinium salt. The second reduction then proceeds in a similar manner to give the tetrahydroisoquinolinium salts. The counter cation of iridium trichloride complex **A** should be changed from isoquinolinium to tetrahydroisoquinolinium according to the progress of the reaction. Based on Crabtree's proposal that the outer-sphere pathway is the most likely hydrogenation mechanism of protonated quinolines by mononuclear iridium trihydride complex **23**,[22,23] it is assumed that hydride attack of the dihydride complex **D** also proceeds through an outer-sphere mechanism. The high enantioselectivity can then be ascribed to the formation of the single isomer of the dihydride complex, which dominantly selected the enantioface of the isoquinolinium chlorides. The chloride counter anion of the substrate interacts with the dihydride complex, as evidenced by the clear dependence of enantiomeric excess on the nature of the counter anion of the substrate salts. Hence, the transition state for hydride attack is proposed to be a six-membered ring, involving the chloride and N-H proton of the substrate salts in a new outer-sphere mechanism.

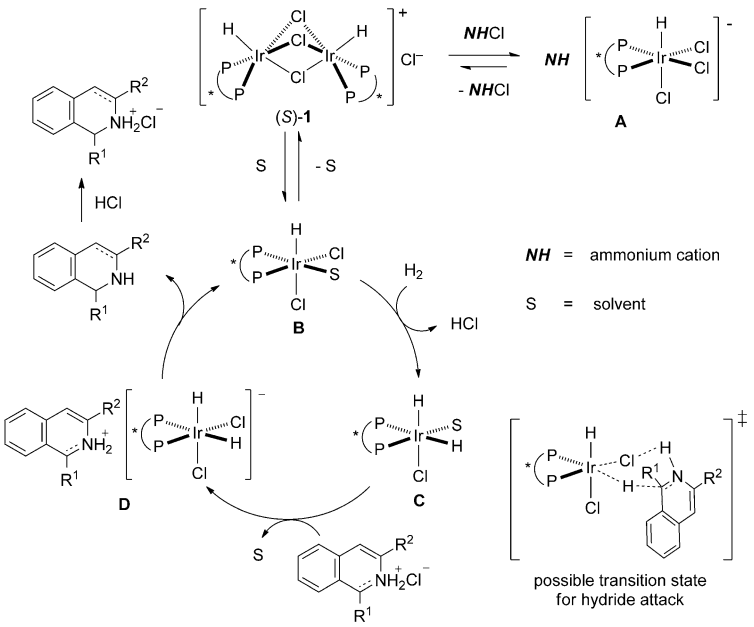

Scheme 11. Proposed catalytic cycle for the asymmetric hydrogenation of isoquinolinium salts.

Conclusion

We have successfully developed the asymmetric hydrogenation of isoquinolines through salt formation prior to hydrogenation using dinuclear iridium complexes (*S*)-**1**, which thus represent useful and versatile catalyst precursors for the synthesis of chiral THIQs with high enantiomeric excess. We have demonstrated that salt formation of the substrate is essential to achieve high yield and high enantioselectivity. Under the optimized conditions, the asymmetric hydrogenation of 1- and 3-substituted isoquinolinium HCl salts proceeded efficiently to afford the desired chiral THIQs in high yields and with high enantioselectivities after simple basic work-up. The construction of two stereogenic centers in a single operation has been achieved by asymmetric hydrogenation of disubstituted isoquinolinium salts. In addition, time-course experiments have revealed that salt formation prevented the catalytic performance and enantioselectivity from being eroded by the negative effects of such substrates and their amine derivatives. Moreover, mechanistic studies, including by ^{1}H and $^{31}P\{^{1}H\}$ NMR and the isolation and characterization of several catalytic intermediates, led to the following observations: (1) chloride coordination to an iridium center prevented the formation of catalytically inactive complex (*S*)-**19**, and (2) iridium dihydride complex (*S*)-**21** is involved in the catalytic cycle. We have proposed a conceptually new transition state involving chloride coordination to an iridium center and a hydrogen bond between the chloride ligand and N-H proton of the substrate salt to form a six-membered outer-sphere ring. Further developments for reducing N-heteroaromatics by the HCl salt formation protocol are being pursued by our group.

Experimental Section

General

All reactions and manipulations involving air- and moisture-sensitive organometallic compounds were performed under argon using standard Schlenk techniques. [{Ir(H)(chiral diphosphine)}$_2$(μ-Cl)$_3$]Cl complexes **1a–d** were prepared according to literature procedures.[13a,24] 1,4-Dioxane was dried and deoxygenated by distillation over sodium benzophenone ketyl under argon, and methanol and ethanol were distilled from the corresponding magnesium alkoxides under argon. *i*PrOH was distilled from calcium hydride. CH_2Cl_2, Et_2O, hexane, THF, and toluene were dried and deoxygenated using a Grubbs column (Glass Counter Solvent Dispensing System, Nikko Hansen & Co., Ltd.). Other chemicals were purchased and used without further purification. ^{1}H NMR (400 MHz), ^{13}C NMR (100 MHz), ^{19}F NMR (376 MHz), and ^{31}P NMR (160 MHz) spectra were measured on a Bruker Avance III-400 spectrometer. All ^{1}H NMR chemical shifts were recorded in ppm (δ) relative to tetramethylsilane or referenced to the chemical shifts of residual solvent resonances ($CHCl_3$ ($\delta_H = 7.26$ ppm) or CH_2Cl_2 ($\delta_H = 5.31$ ppm) were used as internal standards). All ^{13}C NMR chemical shifts were recorded in ppm (δ) relative to $CDCl_3$ ($\delta_C = 77.16$ ppm). ^{31}P NMR chemical shifts were recorded in ppm (δ) relative to 85% H_3PO_4 as an external standard ($\delta_P = 0.00$ ppm). All ^{19}F NMR chemical shifts were recorded in ppm (δ) relative to α,α,α-trifluorotoluene as an external standard ($\delta_F = -63.90$ ppm). UV/Vis spectra were recorded on JASCO UV-2075 or PU-2089 spectrometers. Optical rotations were recorded on a JASCO DIP-370 polarimeter at 589 nm (sodium lamp) and are given in 10^{-1} deg cm^2 g^{-1}. Mass spectra were obtained on Bruker Daltonics MicroTOF II-HB and JEOL JMS-700 spectrometers. All melting points were recorded on a Yanaco micro melting point apparatus. Flash column chromatography was performed on silica gel 60 (40–66.3 μm, 230–400 mesh ASTM). Elemental analyses were performed on a Perkin-Elmer 2400 analyzer at the Faculty of Engineering Science, Osaka University. Hydrogenation reactions were conducted in a TAIATSU stainless steel autoclave or Biotage Endeavor catalyst screening system.

General procedure for asymmetric hydrogenation of isoquinolinium salts

An iridium dinuclear complex (2.4 μmol, 1.0 mol%) and an isoquinolinium salt (0.24 mmol, 1 equiv) were placed in a glass tube in the reactor, and the tube was flushed with argon. A mixed solvent of dry *i*PrOH/1,4-dioxane (1:10; 3 mL) was added through an inlet, and the reactor was charged with H_2 to the desired pressure. The reaction mixture was stirred for 20 h. After releasing the H_2 pressure, the solvent was removed in a rotary evaporator. The residue was poured into saturated aqueous $NaHCO_3$ solution and extracted with ethyl acetate. The organic layer was washed with brine and dried over Na_2SO_4. The conversions were determined by ^{1}H NMR analysis of the products after basic work-up. The enantiomeric excesses were determined by HPLC analysis. Some THIQs had to be acetylated to determine their enantiomeric excesses. For this, a vial was charged with the THIQ (ca. 40 mg), CH_2Cl_2 (2 mL), and triethylamine (3 mL). The reaction mixture was cooled to 0 °C by immersion in an ice bath, whereupon acetyl chloride (3 drops) was added. The reaction mixture was allowed to warm to room temperature and stirred overnight. After filtration through a short pad of silica gel to remove ammonium salts, eluting with ethyl acetate, all volatiles were removed under reduced pressure.

(+)-Methyl 4′-(1,2,3,4-tetrahydroisoquinolin-1-yl)benzoate (3j): Pale-yellow solid; m.p. 93–94 °C; IR (KBr): $\tilde{\nu} = 3335$ (m), 2949 (s), 2803 (s), 1704 (s), 1608 (s), 1573 (w), 1434 (s), 1279 (s), 1112 (s), 1018 cm^{-1} (m); ^{1}H NMR ($CDCl_3$, 400 MHz, 30 °C): $\delta = 8.1$–8.0 (m, 2H), 7.4–7.3 (m, 2H), 7.16 (d, $J = 4.0$ Hz, 2H), 7.1–7.0 (s, 1H), 6.70 (d, $J = 7.8$ Hz, 1H), 5.2 (s, 1H), 3.9 (s, 3H), 3.3–3.2 (m, 1H), 3.1–3.0 (m, 2H), 2.9–2.8 (m, 1H), 2.1 ppm (br s, 1H); ^{13}C NMR (100 MHz, $CDCl_3$, 30 °C): $\delta = 167.1$, 150.1, 137.6, 135.5, 129.9, 129.4, 129.3, 129.1, 128.1, 126.6, 125.9, 61.9, 52.6, 42.3, 29.8 ppm; MS (EI): *m/z*: calcd for $C_{17}H_{17}NO_2$: 267.1259; found: 267.1256; HPLC (Daicel OD-H, hexane/*i*PrOH, 95:5, detector: 215 nm, temperature: 25 °C, flow rate: 1 mL min^{-1}, $t_1 = 20.7$ min, $t_2 = 27.4$ min, major peak t_2); $[\alpha]_{20}^{D} = +31.9$ ($c = 1$, $CHCl_3$).

(+)-1-*p*-Tolyl-1,2,3,4-tetrahydroisoquinoline (3k):[25] Colorless solid; m.p. 79–80 °C; IR (KBr): $\tilde{\nu} = 3441$ (w), 3013 (m), 2970 (m), 1602 (w), 1514 (m), 1491 (s), 1370 (m), 1291 (m), 1121 (s), 1036 cm^{-1} (m); ^{1}H NMR ($CDCl_3$, 400 MHz, 30 °C): $\delta = 7.2$–7.1 (m, 6H), 7.1–7.0 (m, 1H), 6.77 (d, $J = 7.8$ Hz, 1H), 5.1 (s, 1H), 3.3–3.2 (m, 1H), 3.1–3.0 (m, 2H), 2.9–2.8 (m, 1H), 2.3 (s, 3H), 2.2 ppm (br s, 1H); ^{13}C NMR (100 MHz, $CDCl_3$, 30 °C): $\delta = 142.0$, 138.5, 137.0, 135.5, 129.2, 129.1, 128.9, 128.2, 126.3, 125.7, 61.8, 42.3, 29.9, 21.2 ppm; MS (EI): *m/z*: calcd for $C_{16}H_{17}N$: 223.1361; found: 223.1342; HPLC (corresponding acetamide, Daicel OD-H, hexane/*i*PrOH, 99:1, detector: 222 nm, temperature: 28 °C, flow rate: 1 mL min^{-1}, $t_1 = 42.3$ min, $t_2 = 49.9$ min, major peak t_2); $[\alpha]_{20}^{D} = +11.7$ ($c = 1$, $CHCl_3$).

(−)-1-(3-Methoxyphenyl)-1,2,3,4-tetrahydroisoquinoline (3m): Colorless solid; m.p. 105–107 °C; IR (KBr): $\tilde{\nu} = 3420$ (w), 3061 (w), 2912 (m), 1612 (s), 1585 (m), 1492 (s), 1439 (m), 1336 (m),

1278 cm^{-1} (s); ^1H NMR ($CDCl_3$, 400 MHz, 30 °C): δ = 7.3–7.2 (m, 1H), 7.14 (d, J = 4.0 Hz, 2H), 7.1–7.0 (m, 1H), 6.9–6.8 (m, 4H), 5.08 (s, 1H), 3.78 (s, 3H), 3.3–3.2 (m, 1H), 3.1–3.0 (m, 2H), 2.9–2.8 (m, 1H), 1.98 ppm (br s, 1H); ^{13}C NMR (100 MHz, $CDCl_3$, 30 °C): δ = 159.8, 146.6, 138.2, 135.5, 129.5, 129.1, 128.2, 126.4, 125.8, 121.5, 114.8, 112.9, 62.2, 55.3, 42.4, 29.9 ppm; HRMS (EI): *m/z*: calcd for $C_{16}H_{17}NO$: 239.1310; found: 239.1311; HPLC (corresponding acetamide, Daicel OD-H, hexane/*i*PrOH, 95:5, detector: 215 nm, temperature: 10 °C, flow rate: 1 mL min^{-1}, t_1 = 24.3 min, t_2 = 28.2 min, major peak t_1); $[\alpha]_{20}^{D}$ = −123.4 (c = 0.5, $CHCl_3$).

(+)-1-(2-Chlorophenyl)-1,2,3,4-tetrahydroisoquinoline (3n):[26] Pale-yellow oil; IR (neat): $\tilde{\nu}$ = 3328 (w), 3061 (m), 2919 (m), 2830 (w), 1603 (m), 1570 (m), 1493 (s), 1453 (s), 1368 (m), 1292 (s), 1024 cm^{-1} (s); ^1H NMR ($CDCl_3$, 400 MHz, 30 °C): δ = 7.42 (dd, J = 7.8, 1.0 Hz, 1H), 7.2–7.0 (m, 5H), 6.99 (dd, J = 7.5, 1.1 Hz, 1H), 6.77 (d, J = 7.5 Hz, 1H), 5.6 (s, 1H), 3.1–3.2 (m, 1H), 3.1–2.9 (m, 2H), 2.9–2.8 (m, 1H), 2.1 ppm (br s, 1H); ^{13}C NMR (100 MHz, $CDCl_3$, 30 °C): δ = 142.2, 137.2, 135.9, 134.1, 131.2, 129.7, 129.2, 128.5, 128.1, 126.8, 126.5, 125.9, 57.7, 41.4, 29.8 ppm; MS (EI): *m/z*: calcd for $C_{15}H_{14}ClN$: 243.0815; found: 243.0828; HPLC (Daicel OJ-H, hexane/*i*PrOH, 98:2, detector: 215 nm, temperature: 30 °C, flow rate: 0.7 mL min^{-1}, t_1 = 12.7 min, t_2 = 15.2 min, major peak t_2); $[\alpha]_{20}^{D}$ = +17.9 (c = 0.7, $CHCl_3$).

1,3-Diphenyl-1,2,3,4-tetrahydroisoquinoline (5a):[13b] White solid; m.p. 111–112 °C; ^1H NMR ($CDCl_3$, 400 MHz, 30 °C): δ = 7.40 (d, J = 7.3 Hz, 2H), 7.32 (d, J = 6.8 Hz, 2H), 7.3–7.1 (m, 6H), 7.1–6.9 (m, 3H), 6.64 (d, J = 7.8 Hz, 1H), 5.21 (s, 1H), 4.06 (dd, J = 11.0, 3.5 Hz, 1H), 3.1–3.0 (dd, J = 15.8, 11.5 Hz, 1H), 2.92 (dd, J = 15.8, 3.3 Hz, 1H), 2.03 ppm (br s, 1H); ^{13}C NMR ($CDCl_3$, 100 MHz, 30 °C): δ = 144.8, 144.6, 138.7, 135.6, 129.4, 128.9, 128.7, 128.6, 127.8, 127.7, 127.6, 126.8, 126.3, 126.0, 64.5, 59.4, 39.2 ppm; MS (EI^+): *m/z*: calcd for $C_{21}H_{19}N$: 285.1517 $[M-H]^+$; found: 285.1534; HPLC (corresponding trifluoroacetamide, Daicel OD-H, hexane/*i*PrOH, 99:1, detector: 215 nm, flow rate 0.5 mL min^{-1}, t_1 (+) = 15.3 min, t_2 (−) = 16.6 min); $[\alpha]_{20}^{D}$ = +47.8 (c = 1.5, $CHCl_3$) (for an *ee* of 98%).

1-(4-Methoxyphenyl)-3-phenyl-1,2,3,4-tetrahydroisoquinoline (5b): White solid; m.p. 131–133 °C; IR (KBr): $\tilde{\nu}$ = 3310 (w), 3061 (m), 3023 (m), 3003 (m), 2956 (m), 2913 (s), 1612 (s), 1585 (m), 1509 (s), 1493 (s), 1336 (m), 1303 (s), 1173 (s), 1037 (s), 835 cm^{-1} (s); ^1H NMR ($CDCl_3$, 400 MHz, 30 °C): δ = 7.50 (d, J = 7.5 Hz, 2H), 7.4–7.3 (m, 5H), 7.2–7.0 (m, 3H), 6.90 (d, J = 8.5 Hz, 2H), 6.77 (d, J = 7.5 Hz, 1H), 5.25 (s, 1H), 4.23 (dd, J = 11.3, 3.3 Hz, 1H), 3.83 (s, 3H), 3.18 (dd, J = 15.6, 11.5 Hz, 1H), 3.01 (dd, J = 15.8, 3.0 Hz, 1H), 2.06 ppm (br s, 1H); ^{13}C NMR (100 MHz, $CDCl_3$, 30 °C): δ = 159.2, 144.7, 139.1, 137.1, 135.6, 130.4, 128.8, 128.7, 127.7, 127.5, 126.8, 126.3, 125.9, 113.9, 63.8, 59.4, 55.4, 39.2 ppm; MS (EI): *m/z*: calcd for $C_{22}H_{21}NO$: 315.1623; found 315.1627; HPLC (Daicel OD-H, hexane/*i*PrOH, 99:1, detector: 215 nm, temperature: 25 °C, flow rate: 1 mL min^{-1}, t_1 = 10.2 min, t_2 = 19.3 min, major peak t_2); $[\alpha]_{20}^{D}$ = +47.8 (c = 1.5, CH_2Cl_2) (for an *ee* of 96%).

1,3-Bis(4-methoxyphenyl)-1,2,3,4-tetrahydroisoquinoline (5c): White solid; m.p. 204–205 °C; IR (KBr): $\tilde{\nu}$ = 3431 (w), 3000 (m), 2960 (m), 2915 (m), 2837 (m), 1611 (s), 1510 (s), 1302 (s), 1238 (s), 1172 (m), 1035 (s), 833 cm^{-1} (s); ^1H NMR ($CDCl_3$, 400 MHz, 30 °C): δ = 7.38 (m, 4H), 7.2–7.0 (m, 3H), 6.9–6.8 (m, 4H), 6.76 (d, J = 8.0 Hz, 1H), 5.24 (s, 1H), 4.18 (m, 1H), 3.82 (s, 3H), 3.81 (s, 3H), 3.16 (dd, J = 15.3, 11.3 Hz, 1H), 2.97 (m, 1H), 2.07 ppm (br s, 1H); ^{13}C NMR (100 MHz, $CDCl_3$, 30 °C): δ = 159.2, 159.1, 139.1, 137.1, 136.8, 135.7, 130.4, 128.8, 127.9, 127.7, 126.3, 125.9, 114.0, 113.9, 63.9, 58.8, 55.5, 55.4, 39.2 ppm; MS (EI): *m/z*: calcd for $C_{23}H_{24}NO_2$: 346.1807; found: 346.1808; HPLC (Daicel OD-H, hexane/*i*PrOH, 98:2, detector: 215 nm, temperature: 25 °C, flow rate: 1 mL min^{-1}, t_1 = 13.7 min, t_2 = 16.1 min, major peak t_2); $[\alpha]_{20}^{D}$ = +37.3 (c = 1.0, $CHCl_3$) (for an *ee* of 98%).

1,3-Bis(4-methoxycarbonylphenyl)-1,2,3,4-tetrahydroisoquinoline (5d): Yellow solid; m.p. 31–35 °C; IR (KBr): $\tilde{\nu}$ = 3422 (w), 2950 (w), 2368 (w), 2345 (w), 1719 (s), 1434 (m), 1279 (m), 1279 (s), 1175 (w), 1112 (m), 1018 (m), 858 (m), 743 (m), 705 (m), 621 cm^{-1} (w); ^1H NMR ($CDCl_3$, 400 MHz, 30 °C): δ = 8.07–7.99 (m, 4H), 7.62–7.49 (m, 4H), 7.20–7.11 (m, 2H), 7.09–7.02 (m, 1H), 6.69 (d, J = 7.8 Hz, 1H), 5.34 (s, 1H), 4.29 (dd, J = 11.1, 3.5 Hz, 1H), 3.92 (s, 3H), 3.91 (s, 3H), 3.15 (dd, J = 15.6, 11.1 Hz, 1H), 3.00 (dd, J = 15.9, 3.4 Hz, 1H), 2.08 ppm (br, 1H); ^{13}C NMR (100 MHz, $CDCl_3$, 30 °C): δ = 166.9, 166.8, 149.6, 149.3, 137.5, 134.8, 129.9, 129.8, 129.6, 129.4, 129.2, 128.8, 127.4, 126.6, 126.5, 126.0, 63.7, 58.8, 52.0, 38.8 ppm; HRMS (ESI): *m/z*: calcd for $C_{25}H_{24}NO_4^+$: 402.1705 $[M-H]^+$; found: 402.1701; HPLC (Daicel OD-H, temperature: 30 °C, hexane/*i*PrOH, 95:5, detector: 215 nm, flow rate 1.0 mL min^{-1}, t_1 (−) = 21.9 min, t_2 (+) = 24.8 min); $[\alpha]_{20}^{D}$ = +11.5 (c = 0.39, $CHCl_3$) (for an *ee* of 91%).

1-Cyclohexyl-3-phenyl-1,2,3,4-tetrahydroisoquinoline (5e): White solid; m.p. 95–97 °C; IR (KBr): $\tilde{\nu}$ = 3313 (w), 3061 (m), 2925 (s), 2854 (s), 1601 (s), 1563 (m), 1492 (s), 1455 (s), 1306 (m), 1249 (m), 1156 (m), 1028 cm^{-1} (m); ^1H NMR ($CDCl_3$, 400 MHz, 30 °C): δ = 7.55 (d, J = 7.5 Hz, 2H), 7.5–7.4 (m, 2H), 7.3–7.2 (m, 4H), 7.13 (d, J = 7.3 Hz, 1H), 4.30 (s, 1H), 4.04 (dd, J = 11.0, 3.0 Hz, 1H), 3.0–2.8 (m, 2H), 2.1–2.0 (m, 1H), 1.9–1.8 (m, 1H), 1.7–1.6 (m, 4H), 1.5–1.2 ppm (m, 6H); ^{13}C NMR (100 MHz, $CDCl_3$, 30 °C): δ = 145.5, 138.1, 136.9, 128.8, 128.6, 127.4, 126.9, 126.1, 125.7, 125.6, 61.9, 58.0, 44.4, 39.8, 30.9, 27.3, 26.8, 26.7, 25.5 ppm; MS (EI): *m/z*: calcd for $C_{21}H_{26}N$: 292.2065; found 292.2049; HPLC (Daicel OD-H, hexane/*i*PrOH, 99:1, detector: 215 nm, temperature: 15 °C, flow rate: 0.5 mL min^{-1}, t_1 = 9.2 min, t_2 = 10.3 min, major peak t_1); $[\alpha]_{20}^{D}$ = −94.9 (c = 3.0, $CHCl_3$) (for an *ee* of 97%).

3-Hexyl-1-phenyl-1,2,3,4-tetrahydroisoquinoline (5f): Colorless oil; IR (neat): $\tilde{\nu}$ = 3313 (w), 3061 (m), 2925 (s), 2854 (s), 1601 (s), 1563 (m), 1492 (s), 1455 (s), 1306 (m), 1249 (m), 1156 (m), 1028 cm^{-1} (m); ^1H NMR ($CDCl_3$, 400 MHz, 30 °C): δ = 7.4–7.3 (m, 5H), 7.16 (d, J = 4.0 Hz, 2H), 7.1–7.0 (m, 1H), 6.72 (d, J = 7.8 Hz, 1H), 5.15 (s, 1H), 3.2–3.1 (m, 1H), 3.0–2.7 (m, 2H), 1.88 (br s, 1H), 1.7–1.6 (m, 2H), 1.5–1.3 (m, 8H), 0.95 ppm (t, J = 6.8 Hz, 3H); ^{13}C NMR (100 MHz, $CDCl_3$, 30 °C): δ = 144.9, 139.2, 135.7, 129.3, 128.9, 128.6, 127.7, 127.6, 126.2, 125.6, 64.1, 54.6, 37.1, 36.7, 31.9, 29.6, 26.0, 22.7, 14.2 ppm; MS (EI): *m/z*: calcd for $C_{21}H_{27}N$: 293.2144; found: 293.2144; HPLC (Daicel OD-H, hexane/*i*PrOH, 99:1, detector: 215 nm, temperature: 20 °C, flow rate: 0.5 mL min^{-1}, t_1 = 9.3 min, t_2 = 13.3 min, major peak t_1); $[\alpha]_{20}^{D}$ = +18.7 (c = 2.0, $CHCl_3$) (for an *ee* of 98%).

7-Fluoro-1,3-diphenyl-1,2,3,4-tetrahydroisoquinoline (5g): Yellow oil (>95:5 diastereoselectivity); IR (KBr): $\tilde{\nu}$ = 3314 (m), 3085 (m), 3061 (s), 3029 (s), 2924 (m), 2899 (m), 2800 (s), 1613 (s), 1591 (m), 1496 (s), 1455 (s), 1428 (s), 1281 (s), 1254 (s), 1220 (s), 1029 (s), 957 (s), 832 (s), 808 (s), 773 (s), 751 (s), 735 (s), 700 cm^{-1} (s); ^1H NMR ($CDCl_3$, 400 MHz, 30 °C): δ = 7.65–7.27 (m, 5H), 7.08 (t, J = 6.5 Hz, 1H), 6.92–7.68 (m, 1H), 6.52–6.38 (m, 1H), 5.22 (s, 1H), 4.20 (dd, J = 11.2, 2.9 Hz, 1H), 3.18–2.90 (m, 2H), 2.10 ppm (br s, 1H); ^{13}C NMR (100 MHz, $CDCl_3$, 30 °C): δ = 161.0 (d, J = 241.9 Hz), 144.2, 144.0, 140.6 (d, J = 6.6 Hz), 131.0 (d, J = 2.9 Hz), 130.1 (d, J = 7.5 Hz), 129.1, 128.6, 127.8, 127.5, 126.6, 114.0 (d, J = 21.9 Hz), 113.4 (d, J = 21.1 Hz), 64.3 (d, J = 1.6 Hz), 59.2, 38.3 ppm; ^{19}F NMR ($CDCl_3$, 376 MHz, 30 °C): δ = −116.8 ppm; HRMS (ESI): *m/z*: calcd for $C_{21}H_{19}FN^+$: 304.1502 $[M-H]^+$; found: 304.1504; HPLC (Daicel AD-H, temperature: 30 °C, hexane/*i*PrOH, 99:1, detector: 215 nm, flow rate 1.0 mL min^{-1}, t_1 (−) = 15.0 min, t_2 (+) = 23.6 min); $[\alpha]_{20}^{D}$ = +12.8 (c = 1.2, $CHCl_3$) (for an *ee* of 94%).

7-Methoxy-1,3-diphenyl-1,2,3,4-tetrahydroisoquinoline (5h): White solid; m.p. 88–90 °C; IR (KBr): $\tilde{\nu}$ = 3439 (w), 3060 (m), 2829 (m), 1611 (s), 1501 (s), 1454 (s), 1324 (m), 1290 (s), 1257 (s), 1157 (m), 1030 cm^{-1} (s); ^1H NMR (CD_2Cl_2, 400 MHz, 30 °C): δ = 7.50 (d, J = 7.5 Hz, 2H), 7.44 (d, J = 7.0 Hz, 2H), 7.4–7.2 (m, 6H), 7.07 (d, J = 8.5 Hz, 1H), 6.72 (dd, J = 8.5, 2.6 Hz, 1H), 6.27 (s, 1H), 5.25 (s, 1H), 4.19 (dd, J = 11.0, 3.3 Hz, 1H), 3.62 (s, 3H), 3.07 (dd, J = 15.0, 11.0 Hz, 1H), 2.94 (dd, J = 15.6, 3.3 Hz, 1H), 2.05 ppm (br s, 1H); ^{13}C NMR (100 MHz, CD_2Cl_2, 30 °C): δ = 158.1, 145.4, 145.3, 140.2, 130.0, 129.5, 128.9, 128.8, 128.2, 127.9, 127.7, 127.0, 113.3, 112.4, 64.7, 59.7, 55.5, 38.6 ppm; MS (EI): m/z: calcd for $C_{22}H_{21}NO$: 315.1623; found: 315.1606; HPLC (Daicel OD-H, hexane/*i*PrOH, 99:1, detector: 215 nm, temperature: 10 °C, flow rate: 0.4 mL min^{-1}, t_1 = 31.8 min, t_2 = 34.2 min, major peak t_2); $[\alpha]_{20}^{D}$ = −18.9 (c = 1.0, $CHCl_3$) (for an *ee* of 92%).

6-Fluoro-1,3-diphenyl-1,2,3,4-tetrahydroisoquinoline (5i): White solid; m.p. 65–67 °C; IR (KBr): $\tilde{\nu}$ = 3316 (w), 3027 (m), 2827 (m), 1615 (s), 1590 (s), 1495 (s), 1438 (m), 1341 (w), 1280 (s), 1234 (s), 1143 (s), 1028 cm^{-1} (m); ^1H NMR ($CDCl_3$, 400 MHz, 30 °C): δ = 7.50 (d, J = 7.3 Hz, 2H), 7.44 (d, J = 6.8 Hz, 2H), 7.4–7.3 (m, 6H), 6.84 (d, J = 9.0 Hz, 1H), 6.8–6.7 (m, 2H), 5.23 (s, 1H), 4.23 (dd, J = 11.3, 3.3 Hz, 1H), 3.2–3.1 (m, 1H), 2.99 (dd, J = 16.0, 2.8 Hz, 1H), 2.03 ppm (br s, 1H); ^{13}C NMR (100 MHz, $CDCl_3$, 30 °C): δ = 162.5 (d, J = 245.0 Hz), 144.6, 144.2, 137.8 (d, J = 7.3 Hz), 134.6 (d, J = 2.9 Hz), 129.4 (d, J = 8.0 Hz), 129.3, 128.7, 128.6, 127.9, 127.7, 126.8, 115.0 (d, J = 20.5 Hz), 113.1 (d, J = 21.3 Hz), 64.1, 59.2, 39.2 ppm; ^{19}F NMR ($CDCl_3$, 376 MHz, 30 °C): δ = −117.2 ppm; MS (EI): m/z: calcd for $C_{21}H_{18}NF$: 303.1423; found: 303.1404; HPLC (Daicel OD-H, hexane/*i*PrOH, 99:1, detector: 215 nm, temperature: 15 °C, flow rate: 0.5 mL min^{-1}, t_1 = 17.7 min, t_2 = 20.4 min, major peak t_1); $[\alpha]_{20}^{D}$ = + 15.6 (c = 1.0, $CHCl_3$) (for an *ee* of 94%).

6-Methyl-1,3-diphenyl-1,2,3,4-tetrahydroisoquinoline (5j): White solid; m.p. 90–91 °C; IR (KBr): $\tilde{\nu}$ = 3430 (w), 3028 (m), 1614 (m), 1498 (s), 1455 (s), 1354 (w), 1280 (m), 1115 (m), 1026 cm^{-1} (m); ^1H NMR ($CDCl_3$, 400 MHz, 30 °C): δ = 7.50 (d, J = 7.3 Hz, 2H), 7.44 (d, J = 7.0 Hz, 2H), 7.4–7.2 (m, 6H), 6.96 (s, 1H), 6.88 (d, J = 8.0 Hz, 1H), 6.65 (d, J = 7.8 Hz, 1H), 5.26 (s, 1H), 4.22 (dd, J = 11.0, 3.3 Hz, 1H), 3.16 (dd, J = 15.3, 11.3 Hz, 1H), 2.97 (dd, J = 16.0, 3.3 Hz, 1H), 2.31 (s, 3H), 2.01 ppm (br s, 1H); ^{13}C NMR (100 MHz, $CDCl_3$, 30 °C): δ = 145.1, 144.7, 135.9, 135.8, 135.4, 129.4, 129.3, 128.6, 128.5, 127.7, 127.6, 127.5, 126.9, 126.8, 64.3, 59.4, 39.2, 21.1 ppm; MS (EI): m/z: calcd for $C_{22}H_{21}N$: 299.1674; found: 299.1703; HPLC (Daicel OD-H, hexane/*i*PrOH, 99:1, detector: 215 nm, temperature: 10 °C, flow rate: 0.5 mL min^{-1}, t_1 = 13.8 min, t_2 = 14.9 min, major peak t_1); $[\alpha]_{20}^{D}$ = + 10.9 (c = 1.5, $CHCl_3$) (for an *ee* of 97%).

***cis*-3,4-Diphenyl-1,2,3,4-tetrahydroisoquinoline (7)**: Pale-blue solid (> 95:5 diastereoselectivity); m.p. 119–121 °C; IR (KBr): $\tilde{\nu}$ = 3752 (m), 3651 (m), 3356 (s), 3025 (s), 2791 (s), 1578 (m), 1492 (s), 1449 (s), 1361 (m), 1112 (m), 933 (m), 743 (s), 700 cm^{-1} (s); ^1H NMR ($CDCl_3$, 400 MHz, 30 °C): δ = 7.27–7.08 (m, 6H), 7.08–6.96 (m, 4H), 6.91–6.84 (m, 2H), 6.60 (d, J = 6.9 Hz, 2H), 4.44 (d, J = 3.9 Hz, 1H), 4.38 (s, 2H), 4.23 (d, J = 3.7 Hz, 1H), 1.91 ppm (br s, 1H); ^{13}C NMR (100 MHz, $CDCl_3$, 30 °C): δ = 142.0, 141.1, 138.2, 135.4, 130.6, 130.3, 127.8, 127.1, 126.8, 126.7, 126.5, 126.4, 126.0, 125.9, 62.1, 50.8, 49.3 ppm; HRMS (ESI): m/z: calcd for $C_{21}H_{20}N^+$: 286.1596 $[M-H]^+$; found 286.1595; HPLC (Daicel OD-H, temperature: 30 °C, hexane/*i*PrOH, 90:1, detector: 215 nm, flow rate 1.0 mL min^{-1}, t_1 = 6.1 min (major), t_2 (−) = 10.1 min (minor)); $[\alpha]_{20}^{D}$ = + 185 (c = 0.46, $CHCl_3$) (for an *ee* of 43%). The relative configuration of **7** was assigned after N-benzylation and comparing the ^1H NMR chemical shifts of the product with literature values.[27]

1,4-Diphenyl-1,2,3,4-tetrahydroisoquinoline (9): Yellow oil (*syn*:*anti*, 4:1); IR (NaCl): $\tilde{\nu}$ = 3081 (m), 3060 (s), 3025 (s), 2945 (s), 2880 (m), 2808 (m), 2787 (m), 1600 (s), 1580 (m), 1492 (s), 1451 (s), 1367 (m), 1315 (m), 1283 (m), 1259 (m), 1241 (m), 1217 (s), 1179 (m), 1121 (m), 1075 (m), 1029 (m), 917 (m), 844 (m), 807 cm^{-1} (m); ^1H NMR ($CDCl_3$, 400 MHz, 30 °C): *cis*-**9**: δ = 7.41–6.98 (m, 13H), 6.92–6.87 (m, 1H), 5.26 (s, 1H), 4.19 (t, J = 4.6 Hz, 1H), 3.41 (dd, J = 7.7, 5.0 Hz, 1H), 3.25 ppm (dd, J = 7.9, 4.8 Hz, 1H); *trans*-**9**: δ = 7.41–6.98 (m, 13H), 6.81–6.78 (m, 1H), 5.19 (s, 1H), 4.33 (t, J = 8.3 Hz, 1H), 3.49 (dd, J = 6.8, 5.6 Hz, 1H), 3.14 ppm (dd, J = 3.5, 8.8 Hz, 1H); ^{13}C NMR (100 MHz, $CDCl_3$, 30 °C): δ = 145.5, 144.5, 138.5, 137.7, 130.4, 129.6, 129.1, 129.0, 129.0, 128.5, 128.4, 128.0, 127.8, 127.5, 127.4, 126.6, 126.5, 126.4, 126.4, 126.2, 62.6, 62.0, 51.4, 49.8, 46.2, 44.9 ppm; HRMS (ESI): m/z: calcd for $C_{21}H_{20}N^+$: 286.1596 $[M-H]^+$; found: 286.1600; HPLC (*syn*-**9**: Daicel OD-H, temperature: 30 °C, hexane/*i*PrOH, 99:1, detector: 215 nm, flow rate 1.0 mL min^{-1}, t_1 = 13.8 min, t_2 = 16.0 min; *anti*-**9**: Daicel OD-H, temperature: 30 °C, hexane/*i*PrOH, 98.5:1.5, detector: 215 nm, flow rate 1.0 mL min^{-1}, t_1 = 14.3 min, t_2 = 16.8 min); $[\alpha]_{20}^{D}$ = −8.0 (c = 1.1, $CHCl_3$) (for an *ee* of 90% *ee* and 97% *ee* mixture). The relative configuration of **9** was assigned after N-tosylation and comparing the ^1H NMR chemical shifts of the product with literature values.[28]

$Ir(H)_2Cl${(*S*)-binap}(2-methylpyridine) ((*S*)-21): A mixture of $[IrCl(coe)_2]_2$ (353 mg, 0.394 mmol, 1 equiv) and (*S*)-BINAP (503 mg, 0.808 mmol, 2.05 equiv) in toluene was stirred overnight at room temperature. After removing the displaced coe under reduced pressure, 2-methylpyridine (12 equiv) was added and the mixture was stirred for several hours. Under H_2 atmosphere, the color of the solution immediately turned from red to yellow. After the reaction mixture had been stirred overnight, all volatiles were removed under reduced pressure. The residue was redissolved in dichloromethane, and then precipitation by adding hexane afforded (*S*)-**21** as a yellow solid. M.p. 106 °C (decomp.); IR (KBr): $\tilde{\nu}$ = 2962 (m), 2917 (m), 2849 (m), 2363 (w), 1539 (w), 1260 (s), 1093 (s), 1019 (s), 798 cm^{-1} (s); ^1H NMR ([D_8]dioxane, 400 MHz): δ = 9.16 (s, 1H), 8.35 (m, 2H), 8.2–6.0 (m, 33H), 2.91 (s, 3H), −9.41 (dd, J(P,H) = 160, 16 Hz, 1H), −20.6 ppm (t, J(P,H) = 15 Hz, 1H); $^{31}P\{^1H\}$ NMR (161 MHz, [D_8]dioxane, 30 °C): δ = 15.6 (s), 2.22 ppm (s); elemental analysis calcd (%) for $C_{50}H_{41}ClIrNP_2 \cdot 1.5\,CH_2Cl_2$: C 57.65, H 4.13, N 1.31; found: C 57.63, H 4.08, N 1.32.

$Ir(H)_2Cl${(*S*)-segphos}(4-methoxypyridine) ((*S*)-22): The title complex was synthesized according to a similar procedure as used for (*S*)-**21**. The product was recrystallized from Et_2O/CH_2Cl_2 and was obtained as a yellow solid. IR (KBr): $\tilde{\nu}$ = 2962 (m), 2917 (m), 2849 (m), 2539 (w), 1575 (w), 1538 (w), 1260 (s), 1092 (s), 1019 (s), 799 cm^{-1} (s); ^1H NMR (CD_2Cl_2, 400 MHz, 30 °C): δ = 8.68 (s, 2H), 8.5–5.8 (m, 30H), 3.72 (s, 3H), −8.61 (dd, J(P,H) = 160, 18 Hz, 1H), −21.3 ppm (t, J(P,H) = 16 Hz, 1H); $^{31}P\{^1H\}$ NMR (161 MHz, CD_2Cl_2, 30 °C): δ = 8.13 (s), 0.30 ppm (s); elemental analysis calcd (%) for $C_{44}H_{37}ClIrNO_5P_2 \cdot 1.5\,CH_2Cl_2$: C 50.75, H 3.74, N 1.30; found: C 50.38, H 3.63, N 1.37.

X-ray crystallographic analysis

A crystal of (*S*)-**22** was mounted on a CryoLoop (Hampton Research Corp.) with a layer of light mineral oil and placed in a nitrogen stream at 113(1) K. Measurements were made on a Rigaku AFC7R/Mercury CCD detector with graphite-monochromated $Mo_{K\alpha}$ (0.71075 Å) radiation. Crystal data and structure refinement parameters are listed in the Supporting Information.

The structure of (*S*)-**22** was solved by direct methods (SHELXS-97)[29] and refined against F^2 by the full-matrix least-squares method using SHELXS-97. Non-hydrogen atoms were refined anisotropically. H atoms were included in the refinement in calculated positions as riding on their carrier atoms. The function minimized

was $[(F_o^2-F_c^2)^2]$ ($w=1/[\sigma^2(F_o^2)+(aP)^2+bP]$), where $P=(\max(F_o^2,0)+2F_c^2)/3$ with $\sigma^2(F_o^2)$ from counting statistics. The functions R_1 and wR_2 were $(\Sigma||F_o|-|F_c||)/\Sigma|F_o|$ and $[\Sigma w(F_o^2-F_c^2)^2/\Sigma(wF_o^4)]^{1/2}$, respectively. The ORTEP-3 program was used to draw the molecule.[30]

Acknowledgements

This work is financially supported by the Core Research for Evolutionary Science and Technology (CREST) program of the Japan Science and Technology Agency (JST), a Grant-in-Aid for Scientific Research on Innovative Areas "Molecular Activation Directed toward Straightforward Synthesis" from the Ministry of Education, Culture, Sports, Science and Technology (MEXT), Japan, and a Grant-in-Aid for Young Scientists (B) (No. 25810062) from the MEXT, Japan. A.I. expresses his special thanks for the financial support provided by the JSPS Research Fellowship for Young Scientists.

Keywords: asymmetric catalysis · hydrogenation · iridium · nitrogen heterocycles · reaction mechanisms

[1] a) G. Shang, W. Li, X. Zhang, in *Catalytic Asymmetric Synthesis*, 3rd ed. (Ed.: I. Ojima), Wiley, Hoboken, **2010**, Chapter 7, pp. 343 – 436; b) K. Püntener, M. Scalone, W. Bonrath, R. Karge, T. Netcher, F. Roessler, F. Spindler, in *Asymmetric Catalysis on Industrial Scale: Challenges, Approaches and Solutions*, 2nd ed. (Eds.: H. U. Blaser, H. J. Federsel), Wiley-VCH, Weinheim, **2010**, Chapters 2 – 3, pp. 13 – 38.

[2] For reviews, see: a) Y.-G. Zhou, *Acc. Chem. Res.* **2007**, *40*, 1357 – 1366; b) R. Kuwano, *Heterocycles* **2008**, *76*, 909 – 922; c) D.-S. Wang, Q.-A. Chen, S.-M. Lu, Y.-G. Zhou, *Chem. Rev.* **2012**, *112*, 2557 – 2590.

[3] S. Murata, T. Sugimoto, S. Matsuura, *Heterocycles* **1987**, *26*, 763 – 766.

[4] For recent examples, see: a) T. Wang, L.-G. Zhou, Z. Li, F. Chen, Z. Ding, Y. He, Q.-H. Fan, J. Xiang, Z.-X. Yu, A. S. C. Chan, *J. Am. Chem. Soc.* **2011**, *133*, 9878 – 9891; b) Q.-A. Chen, D.-S. Wang, Y.-G. Zhou, Y. Duan, H.-J. Fan, Y. Yang, Z. Zhang, *J. Am. Chem. Soc.* **2011**, *133*, 6126 – 6129; c) J. Qin, F. Chen, Z. Ding, Y.-M. He, L. Xu, Q.-H. Fan, *Org. Lett.* **2011**, *13*, 6568 – 6571; d) T. Wang, G. Ouyang, Y.-M. He, Q.-H. Fan, *Synlett* **2011**, 939 – 942; e) Q.-A. Chen, K. Gao, Y. Duan, Z.-S. Ye, L. Shi, Y. Yang, Y.-G. Zhou, *J. Am. Chem. Soc.* **2012**, *134*, 2442 – 2448; f) N. Ortega, S. Urban, B. Beiring, F. Glorius, *Angew. Chem. Int. Ed.* **2012**, *51*, 1710 – 1713; *Angew. Chem.* **2012**, *124*, 1742 – 1745; g) T. Wang, F. Chen, J. Qin, Y.-M. He, Q.-H. Fan, *Angew. Chem. Int. Ed.* **2013**, *52*, 7172 – 7176; *Angew. Chem.* **2013**, *125*, 7313 – 7317; h) Z.-Y. Ding, T. Wang, Y.-M. He, F. Chen, H.-F. Zhou, Q.-H. Fan, Q. Guo, A. S. C. Chan, *Adv. Synth. Catal.* **2013**, *355*, 3727 – 3735; i) J. Wysocki, N. Ortega, F. Glorius, *Angew. Chem. Int. Ed.* **2014**, *53*, 8751 – 8755; *Angew. Chem.* **2014**, *126*, 8896 – 8900.

[5] For representative examples, see: a) R. Kuwano, K. Sato, T. Kurokawa, D. Karube, Y. Ito, *J. Am. Chem. Soc.* **2000**, *122*, 7614 – 7615; b) M. Studer, C. Wedemeyer-Exl, F. Splindler, H.-U. Blaser, *Monatsh. Chem.* **2000**, *131*, 1335 – 1343; c) C. Bianchini, P. Barbaro, G. Scapacci, *J. Organomet. Chem.* **2001**, *621*, 26 – 33; d) R. Kuwano, K. Kaneda, T. Ito, K. Sato, T. Kurokawa, Y. Ito, *Org. Lett.* **2004**, *6*, 2213 – 2215; e) A. Lei, M. Chen, M. He, X. Zhang, *Eur. J. Org. Chem.* **2006**, 4343 – 4347; f) P. Feiertag, M. Albert, U. Nettekoven, F. Spindler, *Org. Lett.* **2006**, *8*, 4133 – 4135; g) R. Kuwano, M. Kashiwabara, K. Sato, T. Ito, K. Kaneda, Y. Ito, *Tetrahedron: Asymmetry* **2006**, *17*, 521 – 535; h) N. Mršić, T. Jerphagnon, A. J. Minnaard, B. L. Feringa, J. G. de Vries, *Tetrahedron: Asymmetry* **2010**, *21*, 7 – 10; i) A. M. Maj, I. Suisse, C. Méliet, F. Agbossou-Niedercorn, *Tetrahedron: Asymmetry* **2010**, *21*, 2010 – 2014.

[6] For a review, see: Q.-A. Chen, Z.-S. Ye, Y. Duan, Y.-G. Zhou, *Chem. Soc. Rev.* **2013**, *42*, 497–511. For a recent example, see: a) Y. Duan, L. Li, M.-W. Chen, C.-B. Yu, H.-J. Fan, Y.-G. Zhou, *J. Am. Chem. Soc.* **2014**, *136*, 7688 – 7700.

[7] For reviews about additive effects on asymmetric hydrogenation, see: a) Z. Yu, W. Jin, Q. Jiang, *Angew. Chem. Int. Ed.* **2012**, *51*, 6060 – 6072; *Angew. Chem.* **2012**, *124*, 6164 – 6177; b) T. Nagano, A. Iimuro, K. Yamaji, Y. Kita, K. Mashima, *Heterocycles* **2014**, *88*, 103 – 127.

[8] For representative examples of developing chiral diphosphine ligands, see: a) M. Sawamura, H. Hamashima, M. Sugawara, R. Kuwano, Y. Ito, *Organometallics* **1995**, *14*, 4549 – 4558; b) L. Qin, F. Y. Kwong, J. Wu, W. H. Lam, S. Chan, W.-Y. Yu, Y.-M. Li, R. Guo, Z. Zhou, A. S. C. Chan, *J. Am. Chem. Soc.* **2006**, *128*, 5955 – 5965; c) D.-Y. Zhang, D.-S. Wang, M.-C. Wang, C.-B. Yu, K. Gao, Y.-G. Zhou, *Synthesis* **2011**, 2796 – 2802; d) M. Rubio, A. Pizzano, *Molecules* **2010**, *15*, 7732 – 7741; e) S. E. Lyubimov, D. Ozolin, P. Y. Ivanov, A. Melman, V. S. Velezheva, V. A. Davankov, *Chirality* **2014**, *26*, 56 – 60.

[9] For representative examples of developing chiral P,N ligands, see: a) S.-M. Lu, C. Bolm, *Adv. Synth. Catal.* **2008**, *350*, 1101 – 1105; b) A. Baeza, A. Pfaltz, *Chem. Eur. J.* **2010**, *16*, 2036 – 2039; c) D.-S. Wang, J. Zhou, D.-W. Wang, Y.-L. Guo, Y.-G. Zhou, *Tetrahedron Lett.* **2010**, *51*, 525 – 528; d) J. L. Núñez-Rico, J. Fernández-Pérez, J. Benet-Buchholz, A. Vidal-Ferran, *Organometallics* **2010**, *29*, 6627 – 6631.

[10] For an example of developing chiral phosphite and phosphoramidite ligands, see: M. Eggenstein, A. Thomas, J. Theuerkauf, G. Franció, W. Leitner, *Adv. Synth. Catal.* **2009**, *351*, 725 – 732.

[11] For representative examples, see: a) W.-B. Wang, S.-M. Lu, P.-Y. Yang, X.-W. Han, Y.-G. Zhou, *J. Am. Chem. Soc.* **2003**, *125*, 10536 – 10537; b) C. Deport, M. Buchotte, K. Abecassis, H. Tadaoka, T. Ayad, T. Ohshima, J.-P. Genêt, K. Mashima, V. Ratovelomanana-Vidal, *Synlett* **2007**, 2743 – 2747; c) W. Tang, L. Xu, Q.-H. Fan, J. Wang, B. Fan, Z. Zhou, K.-h. Lam, A. S. C. Chan, *Angew. Chem. Int. Ed.* **2009**, *48*, 9135 – 9138; *Angew. Chem.* **2009**, *121*, 9299 – 9302; d) A. M. Maj, I. Suisse, C. Méliet, C. Hardouin, F. Agbossou-Niedercorn, *Tetrahedron Lett.* **2012**, *53*, 4747 – 4750; e) L. Shi, Z.-S. Ye, L.-L. Cao, R.-N. Guo, Y. Hu, Y.-G. Zhou, *Angew. Chem. Int. Ed.* **2012**, *51*, 8286 – 8289; *Angew. Chem.* **2012**, *124*, 8411 – 8414; f) R.-N. Guo, X.-W. Cai, Y.-G. Zhou, *Chem. Commun.* **2013**, *49*, 8537 – 8539.

[12] T. Nagano, A. Iimuro, R. Schwenk, T. Ohshima, Y. Kita, A. Togni, K. Mashima, *Chem. Eur. J.* **2012**, *18*, 11578 – 11592.

[13] a) H. Tadaoka, D. Cartigny, T. Nagano, T. Gosavi, T. Ayad, J.-P. Genêt, T. Ohshima, V. Ratovelomanana-Vidal, K. Mashima, *Chem. Eur. J.* **2009**, *15*, 9990 – 9994; b) A. Iimuro, K. Yamaji, S. Kandula, T. Nagano, Y. Kita, K. Mashima, *Angew. Chem. Int. Ed.* **2013**, *52*, 2046 – 2050; *Angew. Chem.* **2013**, *125*, 2100 – 2104; c) Y. Kita, A. Iimuro, S. Hida, K. Mashima, *Chem. Lett.* **2014**, *43*, 284 – 286.

[14] a) Z. W. Li, T.-L. Wang, Y.-M. He, Z.-J. Wang, Q.-H. Fan, J. Pan, L.-J. Xu, *Org. Lett.* **2008**, *10*, 5265 – 5268; b) N. Mršić, L. Lefort, J. A. F. Boogers, A. J. Minnaard, B. L. Feringa, J. G. de Vries, *Adv. Synth. Catal.* **2008**, *350*, 1081 – 1089; c) N. Mršič, T. Jerphagnon, A. J. Minnaard, B. L. Feringa, J. G. de Vries, *Adv. Synth. Catal.* **2009**, *351*, 2549 – 2552; d) D.-S. Wang, Y.-G. Zhou, *Tetrahedron Lett.* **2010**, *51*, 3014 – 3017.

[15] a) S.-M. Lu, Y.-Q. Wang, X.-W. Han, Y.-G. Zhou, *Angew. Chem. Int. Ed.* **2006**, *45*, 2260 – 2263; *Angew. Chem.* **2006**, *118*, 2318 – 2321; b) Z.-S. Ye, M.-W. Chen, Q.-A. Chen, L. Shi, Y. Duan, Y.-G. Zhou, *Angew. Chem. Int. Ed.* **2012**, *51*, 10181 – 10184; *Angew. Chem.* **2012**, *124*, 10328 – 10331; c) Z.-S. Ye, R.-N. Guo, X.-F. Cai, M.-W. Chen, L. Shi, Y.-G. Zhou, *Angew. Chem. Int. Ed.* **2013**, *52*, 3685 – 3689; *Angew. Chem.* **2013**, *125*, 3773 – 3777.

[16] a) I. Tellitu, D. Badía, E. Domínguez, F. J. García, *Tetrahedron: Asymmetry* **1994**, *5*, 1567 – 1578; b) L. Carrillo, D. Badía, E. Domínguez, F. Ortega, I. Tellitu, *Tetrahedron: Asymmetry* **1998**, *9*, 151 – 155; c) F. A. Davis, Y. W. Andemichael, *J. Org. Chem.* **1999**, *64*, 8627 – 8634; d) J. L. Vicario, D. Badía, E. Domínguez, L. Carrillo, *J. Org. Chem.* **1999**, *64*, 4610 – 4616; e) R. Pedrosa, C. Andrés, J. M. Iglesias, M. A. Obeso, *Tetrahedron* **2001**, *57*, 4005 – 4014; f) S. Chandrasekhar, N. R. Reddy, M. V. Reddy, B. Jagannadh, A. Nagaraju, A. R. Sankar, A. C. Kunwar, *Tetrahedron Lett.* **2002**, *43*, 1885 – 1888; g) M. Dubois, E. Deniau, A. Conture, P. Grandclaudon, *Tetrahedron Lett.* **2012**, *68*, 7140 – 7147; h) J. L. Vicario, D. Badía, L. Carrillo, E. Anakabe, *Tetrahedron: Asymmetry* **2003**, *14*, 347 – 353; i) D. Enders, V. Braig, M. Boudou, G. Raabe, *Synthesis* **2004**, 2980 – 2990; j) T. Kawabata, S. Majumdar, K. Tsubaki, D. Monguchi, *Org. Biomol. Chem.* **2005**, *3*, 1609 – 1611; k) T. Kawabata, S. Matsuda, S. Kawakami, D. Monguchi, K. Moriyama, *J. Am. Chem. Soc.* **2006**, *128*, 15394 – 15395; l) J. M. Concellón, P. Tuya, V. del Solar, S. García-Granda, M. R. Díaz, *Org. Lett.* **2009**, *11*, 3750 – 3753.

[17] D. Zhao, F. Glorius, *Angew. Chem. Int. Ed.* **2013**, *52*, 9616 – 9618; *Angew. Chem.* **2013**, *125*, 9794 – 9796.
[18] a) C.-Y. Legault, A. B. Charette, *J. Am. Chem. Soc.* **2005**, *127*, 8966 – 8967; b) Y.-C. Xiao, C. Wang, Y. Yao, J. Sun, Y.-C. Chen, *Angew. Chem. Int. Ed.* **2011**, *50*, 10661 – 10664; *Angew. Chem.* **2011**, *123*, 10849 – 10852; c) D.-S. Wang, J. Tang, Y.-G. Zhou, M.-W. Chen, C.-B. Yu, Y. Duan, G.-F. Hiang, *Chem. Sci.* **2011**, *2*, 803 – 806; d) ref. [4]; e) Y. Duan, M. W. Chen, Q.-A. Chen, C.-B. Yu, Y.-G. Zhou, *Org. Biomol. Chem.* **2012**, *10*, 1235 – 1238; f) Z.-P. Chen, Z.-S. Ye, M.-W. Chen, Y.-G. Zhou, *Synthesis* **2013**, *45*, 3239 – 3244; g) C. Li, J. Chen, G. Fu, D. Liu, Y. Liu, W. Zhang, *Tetrahedron* **2013**, *69*, 6839 – 6844; h) J. L. Núñez-Rico, H. Fernández-Pérez, A. Vidal-Ferran, *Green Chem.* **2014**, *16*, 1153 – 1157.
[19] a) R. D. Simpson, W. J. Marshall, A. A. Farischon, D. C. Roe, V. V. Grushin, *Inorg. Chem.* **1999**, *38*, 4171 – 4173; b) M. A. Esteruelas, F. J. Fernández-Alvarez, M. Oliván, E. Oñate, *Organometallics* **2009**, *28*, 2276 – 2284.
[20] Two hydrogen bonds between Et_2NH_2Cl and the chloride ligand of a ruthenium complex have been reported, see: T. Ohta, Y. Tonomura, K. Nozaki, H. Takaya, K. Mashima, *Organometallics* **1996**, *15*, 1521 – 1523.
[21] H. Werner, T. Dirnberger, A. Höhn, *Chem. Ber.* **1991**, *124*, 1957 – 1961.
[22] G. E. Dobereiner, A. Nova, N. D. Schley, N. Hazari, S. J. Miller, O. Eisenstein, R. H. Crabtree, *J. Am. Chem. Soc.* **2011**, *133*, 7547 – 7562.
[23] O. Eisenstein, R. H. Crabtree, *New J. Chem.* **2013**, *37*, 21 – 27.
[24] T. Yamagata, H. Tadaoka, M. Nagata, T. Hirao, Y. Kataoka, V. Ratovelomanana-Vidal, J. P. Genêt, K. Mashima, *Organometallics* **2006**, *25*, 2505 – 2513.
[25] M. Chang, W. Li, X. Zhang, *Angew. Chem. Int. Ed.* **2011**, *50*, 10679 – 10681; *Angew. Chem.* **2011**, *123*, 10867 – 10869.
[26] T. Suna, *Chem. Heterocycl. Compd.* **2000**, *36*, 287 – 300.
[27] S. Chandrasekhar, N. R. Reddy, M. V. Reddy, B. Jagannadh, A. Nagaraju, A. Ravi Sankar, A. C. Kunwar, *Tetrahedron Lett.* **2002**, *43*, 1885 – 1888.
[28] S. Wang, Z. Chai, S. Zhou, S. Wang, X. Zhu, Y. Wei, *Org. Lett.* **2013**, *15*, 2628 – 2631.
[29] G. M. Sheldrick, *Acta Crystallogr.* **2008**, *A64*, 112.
[30] L. J. Farrugia, *Appl. Crystallogr.* **1999**, *32*, 837.

Received: September 25, 2014
Published online on November 28, 2014